

**DEVELOPMENT OF ANTIBACTERIAL COATINGS WITH
ENHANCED STABILITY USING REACTIVE EMULSIFIERS IN
STYRENE EMULSION POLYMERIZATION**

by
MINE AYBIKE ERSİN

Submitted to Graduate School of Engineering and Natural Sciences
in partial fulfillment of
the requirements for the degree of Master of Sciences

Sabancı University
December 2024

MİNE AYBIKE ERSİN 2024 ©

All Rights Reserved

ABSTRACT

DEVELOPMENT OF ANTIBACTERIAL COATINGS WITH ENHANCED STABILITY USING REACTIVE EMULSIFIERS IN STYRENE EMULSION POLYMERIZATION

MİNE AYBİKE ERSİN

MATERIALS SCIENCE AND NANO ENGINEERING M.S. THESIS,
DECEMBER 2024

Thesis Supervisor: Prof. Dr. Yusuf Ziya Mencilođlu

Keywords: water-based emulsion, copolymer latex, reactive emulsifier,
antibacterial coating

Polymer latexes and variety of synthetic elastomers are predominantly produced within emulsion polymerization, due to its ability to regulate heat, maintain low viscosity, and control particle size and morphology. The reducing volatile organic compounds (VOC's) have become significant subject of environmental regulations, which increased demand for water-based coatings, making emulsion polymerization a preferred method for their production.

This thesis investigates the synthesis of stable, waterborne styrene copolymer latexes using reactive emulsifiers via emulsion polymerization. The study introduces a novel approach by utilizing both cationic and non-ionic reactive emulsifiers, which impart distinct functionalities to the latex. Cationic emulsifiers enhance the antibacterial properties of latex, while non-ionic emulsifiers improve hydrophilicity and contribute to smooth, transparent surfaces, which are essential for coating applications. A key contribution of this study is the detailed investigation of styrene-based polymerization systems utilizing reactive cationic emulsifiers in the absence of conventional surfactants, thereby addressing a notable gap in existing literature. The copolymer latexes were systematically synthesized, and their structure and property relationships were explored, focusing on latex stability and suitability for antibacterial and transparent coating applications. Variations in emulsifier concentration were studied

to understand their impact on solid content, particle size, and other key properties. A range of analytical techniques were conducted for understanding of physical and thermal properties of the latexes. The results demonstrate that they enhance latex stability, improve uniformity, and optimize the performance of the latex films.

ÖZET

STİREN EMÜLSİYON POLİMERİZASYONUNDA REAKTİF EMÜLGATÖRLER KULLANILARAK STABİLİTESİ ARTTIRILMIŞ, ANTİBAKTERİYEL KAPLAMALARIN GELİŞTRİLMESİ

MİNE AYBİKE ERSİN

MALZEME BİLİMİ VE NANO MÜHENDİSLİK YÜKSEK LİSANS TEZİ,
ARALIK 2024

Tez Danışmanı: Prof. Dr. Yusuf Ziya Menceoğlu

Anahtar Kelimeler: su bazlı emülsiyon, kopolimer lateks, reaktif emülgatör,
antibakteriyel kaplama

Emülsiyon polimerizasyonu, ısı transferi, düşük viskozite, partikül boyutunu ve morfolojisini kontrol etme kabiliyeti nedeniyle sentetik elastomerler ve polimer lateksler dahil olmak üzere çeşitli polimerleri üretmek için yaygın olarak kullanılan bir metottür. Uçucu organik bileşiklerin (UOB) azaltılmasına yönelik artan çevresel düzenlemeler, su bazlı kaplamalara olan talebi daha da artırarak su bazlı emülsiyon polimerizasyonunu tercih edilen bir yöntem haline getirmiştir. Tez çalışması kapsamında, emülsiyon polimerizasyonu yoluyla reaktif emülgatörler kullanılarak stabil, su bazlı stiren kopolimer latekslerin sentezini araştırılmaktadır. Çalışma, latekse farklı işlevler kazandıran hem katyonik hem de iyonik olmayan reaktif emülgatörleri kullanarak yeni bir yaklaşım getirmektedir. Katyonik emülgatörler lateksin antibakteriyel özelliklerini geliştirirken, iyonik olmayan emülgatörler hidrofiliği iyileştirir ve kaplama uygulamaları için gerekli olan pürüzsüz, berrak yüzeylere katkıda bulunur. Bu çalışmaya önemli bir katkı, geleneksel yüzey aktif maddeler içermeyen reaktif katyonik emülgatörler kullanan ve mevcut literatürdeki bir boşluğu dolduran stiren bazlı polimerizasyon sistemlerinin belgelenmesidir. Tez çalışması kapsamında, kopolimer lateksler sistematik olarak sentezlendi. Stabilite, antibakteriyel ve şeffaf kaplama uygulamaları için uygunluğa odaklanarak yapıları ve kimyasal özellik ilişkileri araştırıldı. Emülgatör konsantrasyonundaki varyasyonlar, katı içerik, parçacık boyutu ve diğer temel özellikler üzerindeki etkilerini anlamak için incelenmiştir.

Lateks filmlerin fiziksel ve termal özelliklerini deęerlendirmek için termal analiz ve yüzey karakterizasyonu dahil olmak üzere bir dizi analitik teknik kullanılmıştır. Sonuçlar, reaktif emülgatörlerin lateks stabilitesini önemli ölçüde artırdığını, homojenliği artırdığını ve lateks filmlerin performansını optimize ederek üstün özelliklere sahip gelişmiş su bazlı kaplamaların geliştirilmesi için deęerli bilgiler sağladığını göstermektedir.

ACKNOWLEDGEMENTS

I am deeply appreciative of the continuous encouragement and valuable advice provided by my supervisor, Prof. Dr. Yusuf Ziya Mencelođlu, throughout my master's journey.

I am grateful my thesis committee, Prof. Dr. Ersin Serhatlı and Prof. Dr. Fevzi akmak Cebeci for the curiosity and support. I am deeply appreciate to Assoc. Prof. Nazmiye zlem Őahin, for her generous contributions and collaboration.

I would like to begin by expressing gratitude to my family, my twin, and friends; Havva Duru, İlke Yüksel, my dearest fellows and friends, Işıl Demirkan, Ceren zsaltık, Mustafa Demirer, and Buse Ataç for their unwavering support, for listening to my countless concerns, and for inspiring me to pursue my aspirations.

I am grateful to Dr. Serter Lüleburgaz, Res. Asst. Emre Akar, Dilhan Kandemir, and Bercis Pektaş for their support and comforting me during difficult periods. They have been a valued mentors to me since my bachelor's degree, ensuring that I feel that every accomplishment is significant.

I am appreciated for the assistance of my dearest fellows, including Gizem Arıtürk, Gizem Kurtulmuş, Gökmen Tamer Őanlı, ađla Girişken, Ogeday Rodop, Elif Daldal, Meryem iđdem Uçar, Melike Nur nder.

Lastly, I would like to convey my appreciativeness to Mustafa Kemal Atatürk for guaranteeing that women have equal rights and privileges.

To my family

TABLE OF CONTENTS

LIST OF TABLES	xi
LIST OF FIGURES	xii
LIST OF ABBREVIATIONS	xiii
LIST OF SYMBOLS	xiii
1. INTRODUCTION	1
1.1. The Emulsion Polymerization	1
1.2. Colloidal Stability of a Micelle in Water	3
1.3. Surfactants.....	5
1.3.1. Reactive Surfactants	5
1.3.2. Quaternary Ammonium Compound (QAC).....	6
2. MATERIALS AND METHODS	7
2.1. Materials.....	7
2.2. Synthesis Procedures	7
2.2.1. Synthesis of Non-ionic Emulsifier	7
2.2.2. Synthesis of Cationic Emulsifier.....	8
2.2.3. Synthesis of Styrene Copolymer Latex Using Non-ionic and Cationic Emulsifiers	8
2.2.3.1. Synthesis of P1-19 latex	8
2.2.3.2. Synthesis of P1-24 latex	9
2.2.3.3. Synthesis of P1-35 latex	10
2.2.3.4. Synthesis of P2-19 latex	10
2.2.3.5. Synthesis of P2-24 latex	11
2.2.3.6. Synthesis of P2-35 latex	12
2.3. Characterization of Non-ionic Emulsifier, Cationic Emulsifier, Latex, and Copolymer Film.....	12
2.3.1. Fourier Transform Infrared Spectroscopy(FTIR).....	12

2.3.2.	Scanning Electron Microscopy (SEM).....	13
2.3.3.	Thermal Gravimetric Analysis (TGA)	13
2.3.4.	Differential Scanning Calorimetry Analysis (DSC).....	13
2.3.5.	Water Contact Angle Test	13
2.3.6.	Antibacterial Analysis.....	14
2.3.6.1.	ASTM E2149 20 test	14
2.3.6.2.	In-vitro ISO 22196 test	14
2.3.7.	Gel Permeation Chromatograph Analysis (GPC)	15
2.3.8.	Nuclear Magnetic Resonance (NMR)	15
2.3.9.	Dynamic Light Scattering (DLS).....	16
2.3.10.	UV-VIS Spectroscopy (UV-vis)	16
3.	RESULTS AND DISCUSSION.....	17
3.1.	Preparation of Non- Ionic Emulsifier	17
3.2.	Preparation of Cationic Emulsifier.....	19
3.3.	Preparation of Styrene Copolymer Latex Using Non-ionic and Cationic Emulsifiers.....	20
3.4.	FTIR Analysis	26
3.5.	Morphological Characterization of the Copolymer Latex Films	29
3.6.	Transparency Analysis of Copolymer Latex Films.....	30
3.7.	Contact Angle Measurements	31
3.8.	The Dynamic Light Scattering Analysis of Copolymer Latexes	32
3.9.	Antibacterial Test Analysis	35
3.10.	Thermal Gravimetric Analysis	40
4.	CONCLUSION	48
	BIBLIOGRAPHY.....	49

LIST OF TABLES

Table 3.1. The weight ratio of styrene, copolymer latexes, by using reactive non-ionic emulsifiers and cationic emulsifier.	21
Table 3.2. Optimization of styrene, copolymer latexes by using reactive non-ionic emulsifiers and cationic emulsifier.	22
Table 3.3. Efficiency of copolymer latex film sty/non-ionic emulsifier/cationic emulsifier and molecular weight values.	22
Table 3.4. Particle size distribution profiles 0 th days, 30 days of storage. ...	33
Table 3.5. Antibacterial test of copolymer latexes towards Gram-positive bacteria (<i>S. aureus</i> ATCC 65) by ASTM E2149 standard method. ...	35
Table 3.6. Antibacterial test of copolymer latexes towards Gram negative bacteria (<i>E. coli</i> ATCC 2592) by ASTM E2149 standard method.	36
Table 3.7. Antibacterial test of copolymer latexes towards Gram-positive bacteria (<i>S. aureus</i> ATCC 65) by ISO 22196 standard method.	38
Table 3.8. Antibacterial test of copolymer latexes towards Gram-negative bacteria (<i>E. coli</i> ATCC 2592) by ISO 22196 standard method.	39
Table 3.9. Weight loss of copolymer latex films in TGA.	43
Table 3.10. Thermal properties of copolymer latex films.	47

LIST OF FIGURES

Figure 1.1. The intervals of monomer conversion during emulsion polymerization.	2
Figure 1.2. The colloidal stability of micelle in water a) electrostatic stabilization.	3
Figure 1.3. The colloidal stability of micelle in water b) steric stabilization c) depletion effects.	4
Figure 3.1. Schematic presentation of synthesis of non-ionic emulsifier.	17
Figure 3.2. ¹ H NMR spectrum of non-ionic emulsifier.	18
Figure 3.3. ¹³ C NMR spectrum of non-ionic emulsifier.	18
Figure 3.4. Schematic presentation of synthesis of cationic emulsifier.	19
Figure 3.5. ¹ H NMR spectrum of cationic emulsifier.	19
Figure 3.6. ¹³ C NMR spectrum of cationic emulsifier.	20
Figure 3.7. ¹ H NMR spectrum of P1-19.	23
Figure 3.8. ¹ H NMR spectrum of P1-24.	24
Figure 3.9. ¹ H NMR spectrum of P1-35.	24
Figure 3.10. ¹ H NMR spectrum of P2-19.	25
Figure 3.11. ¹ H NMR spectrum of P2-24.	25
Figure 3.12. ¹ H NMR spectrum of P2-35.	26
Figure 3.13. FTIR spectra of non-ionic emulsifiers and cationic emulsifiers.	27
Figure 3.14. FTIR spectra of copolymer latex films.	28
Figure 3.15. SEM micrographs of copolymer latex films.	29
Figure 3.16. Transmittance values of copolymer latex films.	30
Figure 3.17. Contact angle of copolymer latex films of P1-19, P1-24, P1-35, P2-19, P2-24, P2-35.	32
Figure 3.18. P1-19, P1-24, P1-35, P2-19, P2-24, and P2-35 emulsions on day 30.	33
Figure 3.19. DLS analysis of 0 th day, 30 days of storage.	33

Figure 3.20. The right sample, coated with copolymer latexes, and the left control were assested for their antibacterial efficacy of Gram positive bacteria by ASTM E2149 standard method.....	36
Figure 3.21. The right sample, coated with copolymer latexes, and the left control were assested for their antibacterial efficacy of Gram negative bacteria by ASTM E2149 standard method	37
Figure 3.22. The right sample, coated with copolymer latexes, and the left control were assested for their antibacterial efficacy of Gram positive bacteria by ISO 22196 standard method.	38
Figure 3.23. The right sample, coated with copolymer latexes, and the left control were assested for their antibacterial efficacy of Gram-negative bacteria by ISO 22196 standard method.	39
Figure 3.24. TGA analysis of a) non-ionic emulsifier and b) cationic emulsifier.	40
Figure 3.25. DTA analysis of a) non-ionic emulsifier and b) cationic emulsifier.	41
Figure 3.26. TGA analysis of copolymer latex films.	42
Figure 3.27. DTA analysis of copolymer latex films.	43
Figure 3.28. DSC curves of a) non-ionic emulsifier.	44
Figure 3.29. DSC curves of b) cationic emulsifier	44
Figure 3.30. DSC curves of copolymer latex films a) 1 st heating	46
Figure 3.31. DSC curves of copolymer latex films b) 2 nd heating	47

LIST OF ABBREVIATIONS

- VOC's: Volatile Organic Compounds
- DLS: Dynamic Light Scattering
- TGA: Thermal Gravimetric Analysis
- DSC: Differential Scanning Calorimetry Analysis
- UV-vis: UV-VIS Spectroscopy
- SEM: Scanning Electron Microscopy
- DLVO: Derjaguin, Landau, Verwey, and Overbeek
- V: Potential Energy
- WSP: Water-soluble Polymer
- H: Distance
- SAHS: Sodium Allyl Hydroxyalkyl Sulphate
- AHPS: 3-Allyloxy-2-Hydroxypropanesulfonic Salt
- QAC's: Quaternary Ammonium Compounds
- BAC's: Benzyl Alkyl Dimethyl Ammonium Compounds
- ATMAC's: Alkyl Trimethyl Ammonium Compounds
- DADMAC's: Dialkyl Dimethyl Ammonium Compounds
- D.I water: Distilled Water
- FTIR: Fourier Transform Infrared Spectroscopy
- GPC: Gel Permeation Chromatography Analysis
- NMR: Nuclear Magnetic Resonance

DLS: Dynamic Light Scattering

PEG: Polyethylene Glycol

APS: Ammonium Persulfate

ABVA: Azobis Valeric Acid

V_{max} : Maximum Potential Energy

PDI: Polydispersity Index

BA: Butyl Acrylate

MMA: Methyl Methacrylate

AA: Acrylic Acid

P-TsOH: P-Toluene Sulfonic Acid Monohydrate

NB, Oxoid: Nutrient Broth

SCDLP Broth: Soybean Casein Lecithin Polysorbate Broth

LIST OF SYMBOLS

°C: Celsius Degree

rpm: Revolutions per Minute

g: Gram

h: Hour

Da: Dalton

mL: Milliliter

M_n: Number Average Molecular Weight

M_w: Weight Average Molecular Weight

T_g: Glass Transition Temperature

T_m: Melting Temperature

W_i: Weight Initial

W_f: Weight Final

%: Percentage

mol: Mole

mm: Millimeter

°C/min: Celsius per Minute

min: Minute

nm: Nanometer

g/mol: Gram per Mole

ppm: Parts per Million

wt: Weight

Sty: Styrene

cm^{-1} : Number of Wavelengths per Unit Distance

cfu/mL: Colony Forming per Milliliter

1. INTRODUCTION

1.1 The Emulsion Polymerization

Generating the polymer latexes by emulsion polymerization requires an insoluble monomer within an aqueous surfactant solution. Throughout the process, the surfactant attaches to the surfaces of insoluble monomers, establishing an interface with aqueous media. The interface led to the segregation of insoluble monomers into droplets, referred to as micelles. Micelles are spherical groups that are attached by around 50 to 100 surfactant molecules, with varying amounts according to the concentration of the surfactant. The hydrophobic segments of surfactants, which face inward, side with their hydrophilic segments, which extend into the water phase, leading to the dispersion of the insoluble monomers into aqueous media (Harkins (1947); Ugelstad & Hansen (1976)).

Polymerization begins with the introduction of a soluble radical initiator, leading to the formation of the radical oligomers. Afterwards, radical oligomers penetrate micelles and continue polymerization while simultaneously penetrating the monomer droplets (Hansen & Ugelstad (1978); Lovell & Schork (2020)). Although free radical polymerization is a prominent method to generate high molecular weight polymers, emulsion polymerization yields greater molecular weight polymers (Lovell & Schork (2020)). The presence of propagating polymer chains inside micelles increases the possibility of active site formation; as a result, it inhibits the development of short polymer chains. In addition, a rapid polymerization rate enables high molecular weight as well, making it a key method in comparison to alternative polymerization approaches, such as free radical polymerization (Harkins (1947); Szkurhan & Georges (2004)).

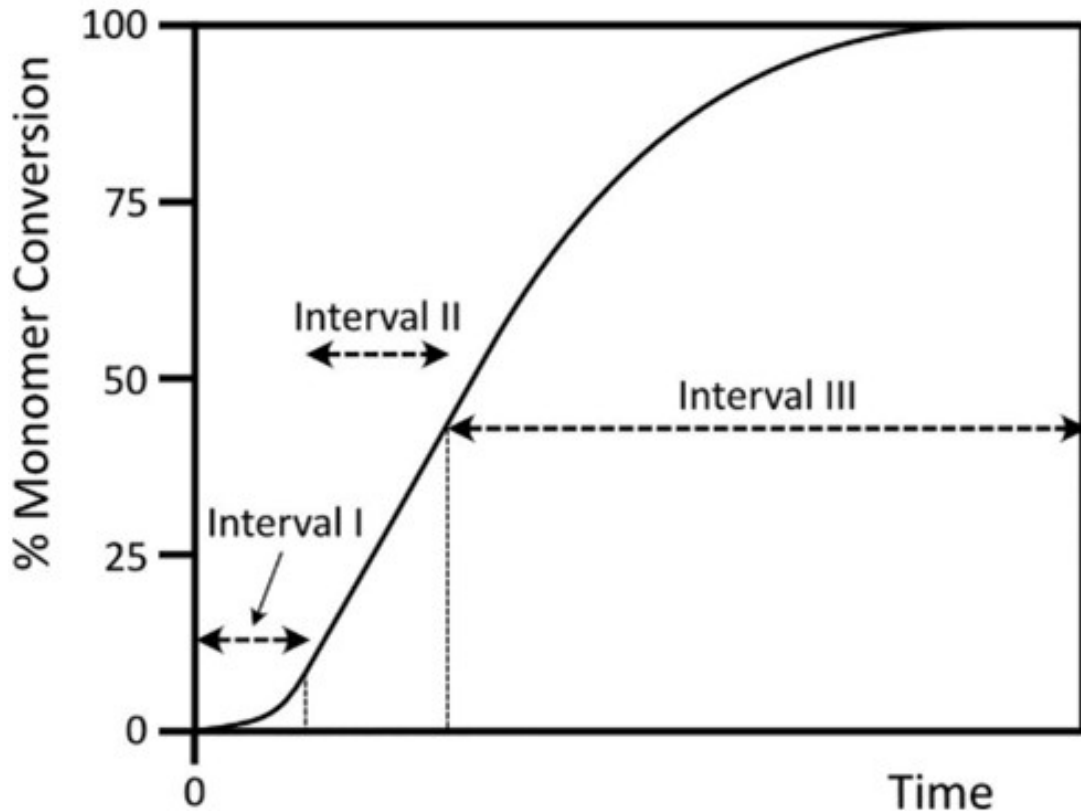


Figure 1.1 The intervals of monomer conversion during emulsion polymerization.

Harkins has outlined the three individual stages of monomer conversion in the emulsion polymerization process, as seen in Figure 1.1. He has identified these stages as Intervals I, II, and III. The interval I stage demonstrates the formation of polymer particles that remain stable and then increase in size by further polymerization. Interval II proceeds, characterized by a steady polymerization rate among monomer micelles. Interval III gradually reduces the polymerization rate as it utilizes the remaining monomer (Lovell & Schork (2020)).

The current understanding of emulsion polymerization incorporates historical developments and rationalizes them with recent insights. To conclude, the hydrophobic monomers disperse in the aqueous phase by the surfactant and are initiated by soluble radicals, through the process active side of the dispersed monomers reacting with other monomers which is leading to polymerization in aqueous media (Friberg (1985)).

1.2 Colloidal Stability of a Micelle in Water

The absence of forces between micelles will lead to the coagulation of colloidal particles. Colloidal stability may be displayed in three distinct forms, as seen in Figure 1.1 and Figure 1.2.

Electrostatic stabilization has the primary impact during emulsion polymerization. Ionic surfactants are contributing to the surface charge of micelles through their headgroup. The surface charge of counterions constituting the electrical double layer and diffuse region are the main factors that ensure colloids are stable. The counterion concentration diminishes at a significant distance from the surface, leading to a force that withdraws the counterions from it (Friberg (1985); Tsuji & Kawaguchi (2005)).

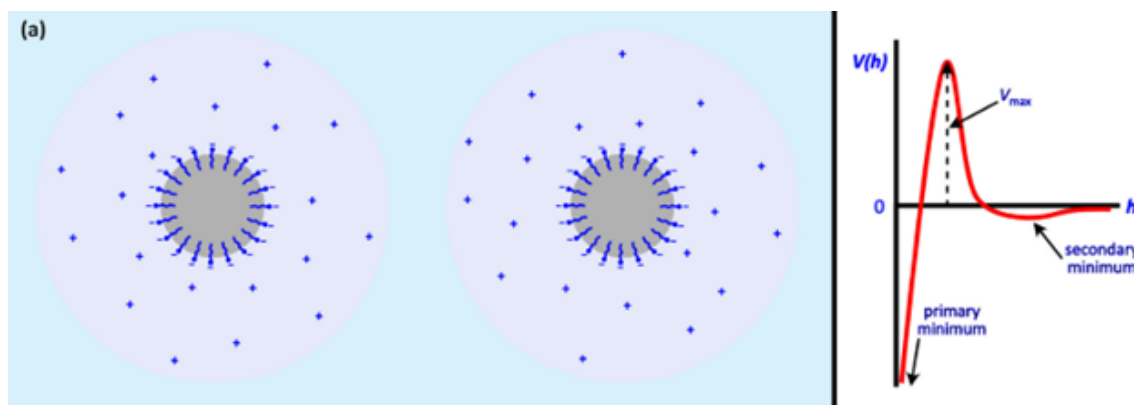


Figure 1.2 The colloidal stability of micelle in water a) electrostatic stabilization.

The Derjaguin, Landau, Verwey, and Overbeek (DLVO) theory illustrates the variation of the sum of the potential energies (V) corresponding of distance between particles (h). (Figure 1.2) In order to provide colloidal stability, maximum potential energy (V_{max}) should surpass $10 kT$. Introducing ions into the water phase may greatly reduce the diffuse region of counterions and increase V_{max} , hence compromising colloidal stability. Apparently, particles that can overcome the potential energy barrier undergo the process known as coagulation. Steric stabilization occurs when micelle surface is covered with water-soluble polymer (WSP) chains that extend into the aqueous phase. Since no repulsive force exists between particles, they may approach within the surface layer of polymer chains, which polymer-water interactions are preferred.

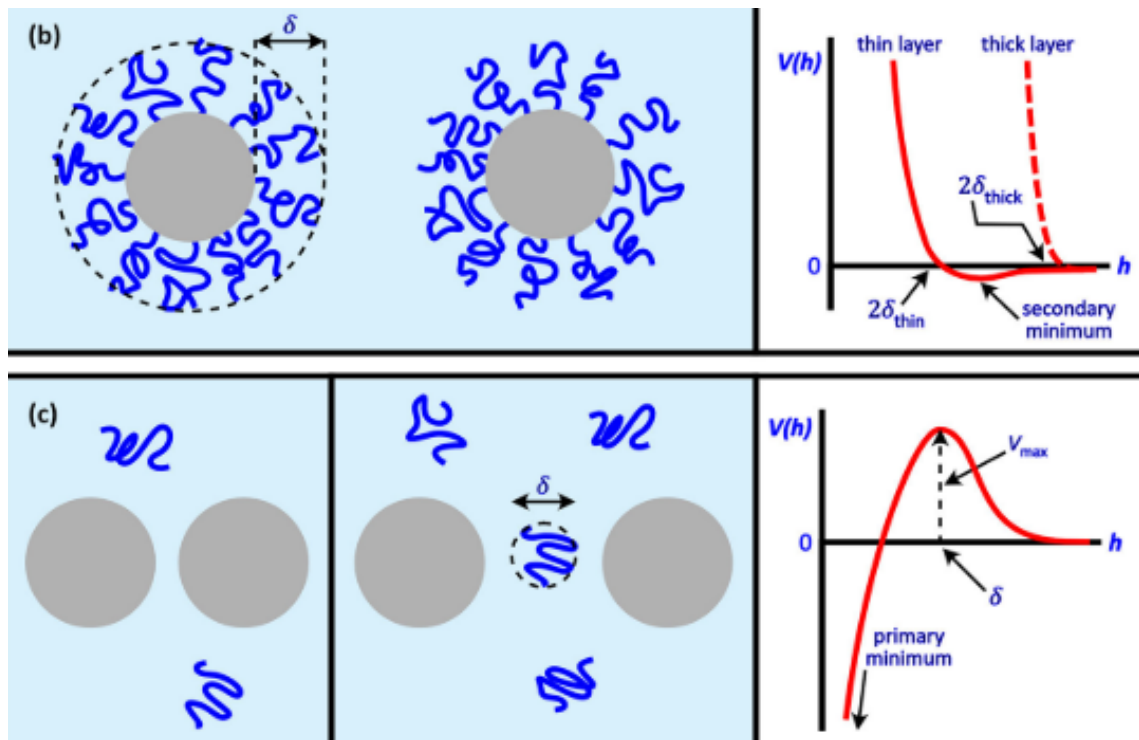


Figure 1.3 The colloidal stability of micelle in water b) steric stabilization c) depletion effects.

Electrosteric stabilization is incorporated with steric and electrostatic stabilization by adsorbing charged polymer chains onto the micelle surface. Nonetheless, the adsorbed chains may collapse onto the surface if solvency conditions diminish. While if it changes, the chain will grow, which disintegrates the micelle into a stable colloidal form (Friberg (1985); Tsuji & Kawaguchi (2005)).

Depletion effects arose from free polymer chains in the aqueous media, which can be challenging to comprehend due to their high probability of permitting particles to approach one another. At lower concentrations of polymer chains, micelles are more likely to contact each other without a chain between them. At higher concentrations of polymer chains, the particles become concentrated and the area between them, creates a repulsive force. This results in potential energy that lacks surface charges or adsorbed polymer chains.

Depletion stabilization occurs when particles have a maximum energy barrier. The aggregation can still be undone because the adsorbed polymer chains inhibit the direct contact of micelle surfaces with each other (Tsuji & Kawaguchi (2005)).

1.3 Surfactants

Surfactants are crucial for stabilizing emulsions by enhancing the compatibility between the oil and water phases. However, excessive surfactants can lead to overly stable emulsions, which increase viscosity and disrupt the flow. The type of surfactant, whether anionic, cationic, or non-ionic, affects the charge distribution at the interface, thereby influencing emulsion stability. Additionally, variations in temperature and pH can alter surfactant behavior and interfacial forces, further impacting stability. In emulsion polymerization, surfactants are polymerized through free radical polymerization of monomers such as acrylate and acrylic acid, using peroxides as initiators (Aramendia, Mallégol, Jeynes, Barandiaran, Keddie & Asua (2003); Goel, Beginn, Mourran & Moller (2008)).

Gemini surfactants, which have a reduced surface tension, exhibit exceptional catalytic properties, and low critical micelle concentration shows considerable potential for further research. Similarly, amine-functionalized polysiloxanes, known for their low critical micelle concentration, also demonstrate promising catalytic capabilities, making them an essential avenue for future studies (Goel et al. (2008); Zhang, Wang, Dai, Pan, Zhang & He (2011)).

1.3.1 Reactive Surfactants

Reactive surfactants, including commercial macromonomers, have been developed to replace traditional adsorbed surfactants in emulsion polymerization. These surfactants possess both hydrophilic and hydrophobic properties and serve dual functions during polymerization, acting as surfactants and comonomers. By reducing the movement of surfactant molecules during film formation, it may enhance the stability of the resulting latex.

The role of reactive surfactants in emulsion polymerization has been studied by Aramendia et al. (2003) extensively. In study of atomic force microscopy, it has demonstrated that reactive surfactants effectively prevent unwanted surfactant exudation in acrylic latex films (Chang, Liu, Zhang, Pan & Pei (2009)). These surfactants can be readily incorporated into the latex through copolymerization, resulting in higher surface tension. However, the mechanisms of particle agglomeration remain insufficiently understood and require further investigation. Furthermore, emulsion

polymerization using surfactants is typically conducted under conditions with relatively low solid content (Aramendia et al. (2003); Goel et al. (2008)).

Reactive emulsifiers, serving both as comonomers and emulsifiers, have garnered significant interest among scientists. For instance, Chang et al. (2009) documented the use of sodium allyl hydroxyalkyl sulphonate (SAHS) in the MMA/BA/AA monomer system. Tang Guangliang demonstrated the application of 3-allyloxy-2-hydroxypropanesulfonic acid (AHPS) in the MMA-BA monomer system (Zhang et al. (2011)). Additionally, Hu et al. reported the use of the Er-30 composite system and Se-10N composite system as a reactive emulsifier in the formulation of acrylate emulsion as an adhesive (Chang et al. (2009)).

1.3.2 Quaternary Ammonium Compound (QAC)

Quaternary ammonium compounds are classified as cationic surfactants with bactericidal properties. A fundamental QAC structure is made up of a positively charged nitrogen atom connected to at least one hydrophobic hydrocarbon chain, mainly alkyl groups. The amphiphilic properties of quaternary ammonium compounds are controlled by the halogen anions that are present in most of them. Environmental research often uses QAC. Some examples are alkyltrimethyl ammonium compounds (ATMACs), dialkyl dimethyl ammonium compounds (DADMACs), and benzylalkyldimethyl ammonium compounds (BACs). Benzalkonium chloride is a quaternary ammonium compound employed as an antibacterial preservative in pharmaceutical formulation. The alkyl chain of benzalkonium chloride attributes the biocidal effectiveness of it. The prior mechanism of inhibition of microbial activities are by disruption of intermolecular bonds, which exhibit microbicidal properties for QACs (Goel et al. (2008), Watrobska-Swietlikowska (2020), Mohapatra, Xian, Galvez-Rodriguez, Ekande, Drewes & Gin (2024)). Another approach is dissociation of cellular membrane lipid bilayers, which is compromising cellular permeability control and resulting in the leakage of cellular contents (Mohapatra et al. (2024)).

2. MATERIALS AND METHODS

2.1 Materials

1-octadecanol (95%, Aldrich), maleic anhydride (99%, Aldrich), polyethylene glycol 2,000 (PEG 2000, Alfa Aesar), *p*-toluene sulfonic acid monohydrate (*p*TsOH, 97%, Alfa Aesar), 4-vinyl benzyl chloride (90%, Aldrich), *N,N*-dimethyldodecylamine (97%, Aldrich), ammonium persulfate (APS, Aldrich), 4,4-azobis(4-cyanovaleric acid) ($\geq 98\%$, Aldrich), styrene (99.9%, Aldrich) was distilled over a column of alumina. Chloroform (CHCl_3 , $\geq 99\%$, Aldrich) and toluene (99.8%, Sigma-Aldrich), were anhydrous and used without further purification. Ethyl acetate and methanol were reagent grade and used without further purification.

2.2 Synthesis Procedures

2.2.1 Synthesis of Non-ionic Emulsifier

A non-ionic emulsifier was synthesized following a reported procedure (Solyman, Elsharaky & El-Tabey (2018)).

^1H NMR (CDCl_3 , δ): 6.06 (s, 2H, $\text{O}=\text{CCHCHC}=\text{O}$), 4.15 (s, 2H, $\text{O}=\text{COCH}_2\text{CH}_2\text{O}$), 3.57 (s, 17H, $\text{O}=\text{COCH}_2\text{CH}_2\text{OCH}_2\text{CH}_2\text{OCH}_2\text{CH}_2\text{OH}$, PEG chain), 1.61 (s, 6H, $\text{O}=\text{COCH}_2\text{CH}_2\text{CH}_2\text{CH}_2$), 1.19 (s, 28H,

O=COCH₂CH₂CH₂CH₂CH₂, alkyl chain of alcohol), 0.81 (s, 3H, terminal proton of alcohol chain).

¹³C NMR (CDCl₃, δ): 165.3, 134.3, 77.3, 70.4, 66.5, 64.4, 61.4, 31.9, 29.6, 22.6, 14.

2.2.2 Synthesis of Cationic Emulsifier

N,N-dimethyldodecylamine (16.17 g, 0.06 mol, 1 equiv) was dissolved in a total of 25 mL DI water into a round-bottom flask, and was stirred 75°C for 3 hours. Meanwhile, vinyl benzyl chloride (9.15 g, 0.06 mol, 1 equiv) was added into the system drop wisely within 1 hour. After the specified reaction time, the mixture in the water layer was extracted with 20 mL of ethyl acetate, repeated three times. The solvent was removed by a rotary evaporator. The obtained quarternize ammonium sample was a sustained yellowish liquid. (Yield= 41.44 g, 82.88%)

¹H NMR (CDCl₃, δ): 7.56 (d, 2H, ArH), 7.35 (d, 2H, ArH), 6.61 (q, 1H, ArCHCH₂), 5.74 (t, 1H, ArCHCH₂), 5.26 (t, 1H, ArCHCH₂), 4.96 (s, 2H, ArCH₂N), 3.46 (d, 2H, NCH₂, alkyl chain), 3.21 (s, 6H, CH₃N, methyl group), 1.72 (s, 2H, NCH₂CH₂), 1.17 (m, 2H, NCH₂CH₂CH₂), 0.80 (t, 3H, NCH₂CH₂CH₂CH₃).

¹³C NMR (CDCl₃, δ): 139.6, 135.5, 133.6, 126.7, 116, 67, 63.4, 49.4, 29.2, 26.3, 22.8, 22.5, 14.

2.2.3 Synthesis of Styrene Copolymer Latex Using Non-ionic and Cationic Emulsifiers

2.2.3.1 Synthesis of P1-19 latex

Styrene-copolymer latex with non-ionic emulsifier, and cationic emulsifier, named as P1-19, was prepared via four steps; 1-) Non-ionic surfactant (1.025 g, 0.0005 mol) and cationic surfactant (1.025 g, 0.0031 mol) and 20 mL DI water were poured in a beaker and stirred at 60°C. Afterward, styrene (17 g, 0.16 mol) was poured to the mixture, dropped wisely, and stirred for 30 minutes 2-) Non-ionic surfactant (1.025g, 0.0005 mol), cationic surfactant (1.025 g, 0.0031 mol), and 20 mL DI water, stirred

in a beaker, then poured into 250 mL four-necked round bottom flask with condenser and thermocouple, was stirred at 300 rpm 75°C. The system was degassed for 30 minutes. 3-) The pre-emulsion was poured into an addition funnel and fed to the reaction mixture for 4 hours. Simultaneously, the aqueous solution of APS (0.17 g, 10 mL DI water) was also fed to the mixture. The emulsion was heated to 80°C and stirred at 300 rpm. 4-) After the feeding, the reaction was stirred at 75°C for 2 hours. Post-procedure—The latex was filtered through a 300-mesh filter.

(Monomer conversion = 42.45%, $M_{n, GPC} = 1095000$ Da, $M_w/M_n = 1.78$).

$^1\text{H NMR}$ (CDCl_3 , δ): 7.10 (s, 2H, ArH, styrene), 7.05 (s, 3H, ArH, styrene), 6.59 (s, 2H, ArH, cationic emulsifier), 6.47 (s, 2H, ArH, cationic emulsifier), 3.66 (s, 171H, $\text{O}=\text{COCH}_2\text{CH}_2\text{OCH}_2\text{CH}_2\text{OCH}_2\text{CH}_2\text{OH}$, PEG chain), 2.75 (s, 1H, $\text{O}=\text{CHCH}=\text{O}$, maleic anhydride), 1.27 (m, 28H, $\text{O}=\text{COCH}_2\text{CH}_2\text{CH}_2\text{CH}_2$, alkyl chain of alcohol), 0.88 (s, 6H, $\text{NCH}_2\text{CH}_2\text{CH}_2\text{CH}_3$, terminal proton of alcohol chain).

2.2.3.2 Synthesis of P1-24 latex

Styrene-copolymer latex with non-ionic emulsifier and cationic emulsifier, named P1-24, was prepared via four steps: 1-) Non-ionic emulsifier (1.37 g, 0.00065 mol) and cationic emulsifier (1.37 g, 0.004 mol) and 22 mL DI were poured in a beaker and stirred at 60°C. Afterward, styrene (17 g, 0.16 mol) was poured to the mixture, dropped wisely, and stirred for 30 minutes. 2-) Non-ionic emulsifier (1.037 g, 0.00065 mol), and cationic emulsifier (1.37 g, 0.004 mol), and 21 mL DI water, stirred in a beaker, then poured into 250 mL four-necked round-bottomed flask with a condenser and thermocouple, was stirred at 300 rpm 75°C. The system was degassed for 30 minutes. 3-) The pre-emulsion was poured into an addition funnel and fed to the reaction mixture for 4 hours. Simultaneously, the aqueous solution of APS (0.17 g, 10 mL DI water) was also fed to the reaction mixture. The emulsion was stirred at 300 rpm 80°C. 4-) After the feeding, the reaction was stirred at 75°C for 2 hours. Post-procedure, the latex was filtered through a 300-mesh filter.

(Monomer conversion = 42.45%, $M_{n, GPC} = 2080000$ Da, $M_w/M_n = 1.45$).

$^1\text{H NMR}$ (CDCl_3 , δ): 7.09 (s, 2H, ArH, styrene), 7.04 (s, 3H, ArH, styrene), 6.57 (s, 2H, ArH, cationic emulsifier), 6.46 (s, 2H, ArH, cationic emulsifier), 3.65 (s, 171H, $\text{O}=\text{COCH}_2\text{CH}_2\text{OCH}_2\text{CH}_2\text{OCH}_2\text{CH}_2\text{OH}$, PEG chain), 2.79 (s, 1H, $\text{O}=\text{CHCH}=\text{O}$, maleic anhydride), 1.26 (m, 28H, $\text{O}=\text{COCH}_2\text{CH}_2\text{CH}_2\text{CH}_2$, alkyl chain of alcohol), 0.88 (s, 6H, $\text{NCH}_2\text{CH}_2\text{CH}_2\text{CH}_3$, terminal proton of alcohol chain).

2.2.3.3 Synthesis of P1-35 latex

Styrene-copolymer latex with non-ionic emulsifier, and cationic emulsifier, named P1-35, was prepared via four steps; 1-) Non-ionic emulsifier (2.30 g, 0.001 mol) and cationic emulsifier (2.30 g, 0.007 mol) and 26 mL DI water were poured in a beaker and stirred at 60°C. Afterward, styrene (17 g, 0.16 mol) was poured to the mixture, dropped wisely, and stirred for 30 minutes. 2-) Non-ionic emulsifier (2.30 g, 0.001 mol), and cationic emulsifier (2.30 g, 0.007 mol) and 25 mL DI water, stirred in a beaker, then poured into 250 mL four-necked bottom flask with condenser and thermocouple, was stirred at 300 rpm at 75°C. The system was degassed for 30 minutes. 3-) The pre-emulsion was poured into an addition funnel and fed to the reaction mixture for 4 hours. Simultaneously, the aqueous solution of APS (0.17 g, 10 mL DI water) was also fed to the reaction mixture. The emulsion was stirred at 300 rpm 80°C. 4-) After feeding, the reaction was stirred at 75°C for 2 hours. Post-procedure: The latex was filtered through a 300-mesh filter.

(Monomer conversion = 42.45%, $M_{n, \text{GPC}} = 1796000$ Da, $M_w/M_n = 1.3$).

$^1\text{H NMR}$ (CDCl_3 , δ): 7.09 (s, 2H, ArH, styrene), 7.05 (s, 3H, ArH, styrene), 6.58 (s, 2H, ArH, cationic emulsifier), 6.46 (s, 2H, ArH, cationic emulsifier), 3.65 (s, 171H, $\text{O}=\text{COCH}_2\text{CH}_2\text{OCH}_2\text{CH}_2\text{OCH}_2\text{CH}_2\text{OH}$, PEG chain), 2.70 (s, 1H, $\text{O}=\text{CHCH}=\text{O}$, maleic anhydride), 1.27 (m, 28H, $\text{O}=\text{COCH}_2\text{CH}_2\text{CH}_2\text{CH}_2$, alkyl chain of alcohol), 0.90 (s, 6H, $\text{NCH}_2\text{CH}_2\text{CH}_2\text{CH}_3$, terminal proton of alcohol chain).

2.2.3.4 Synthesis of P2-19 latex

Styrene-copolymer latex with non-ionic emulsifier, and cationic emulsifier, named P2-19, was prepared via four steps: 1-) Non-ionic emulsifier (1.025 g, 0.0005 mol), cationic emulsifier (1.025 g, 0.0031 mol), the aqueous solution of ABVA (0.17 g, 10 mL DI water), and 20 mL DI water were poured in a beaker and stirred at 60°C. Afterward, styrene (17 g, 0.16 mol) was poured to the mixture, dropped wisely, and stirred for 30 minutes. 2-) Non-ionic emulsifier (1.025g, 0.0005 mol) and cationic emulsifier (1.025g, 0.0031 mol) and 20 mL DI water, stirred in a beaker, then poured into a 250 mL three-necked round-bottomed flask with condenser, and thermocouple, was stirred at 300 rpm and at 75°C. The system was degassed for 30 minutes. 3-) The pre-emulsion was poured into an additional funnel and fed to the reaction mixture for 4 hours. The emulsion was stirred at 300 rpm 80°C. 4-) After the feeding, the reaction was stirred at 75°C for 2 hours. Post-procedure: The latex

was filtered through a 300-mesh filter.

(Monomer conversion = 42.45%, $M_{n, \text{GPC}} = 4545000$ Da, $M_w/M_n = 1.3$).

$^1\text{H NMR}$ (CDCl_3 , δ): 7.10 (s, 2H, ArH, styrene), 7.05 (s, 3H, ArHH, styrene), 6.58 (s, 2H, ArH, cationic emulsifier), 6.47 (s, 2H, ArH, cationic emulsifier), 3.66 (s, 171H, $\text{O}=\text{COCH}_2\text{CH}_2\text{OCH}_2\text{CH}_2\text{OCH}_2\text{CH}_2\text{OH}$, PEG chain), 2.73 (s, 1H, $\text{O}=\text{CHCH}=\text{O}$, maleic anhydride), 1.27 (m, 28H, $\text{O}=\text{COCH}_2\text{CH}_2\text{CH}_2\text{CH}_2$, alkyl chain of alcohol), 0.90 (s, 6H, $\text{NCH}_2\text{CH}_2\text{CH}_2\text{CH}_3$, terminal proton of alcohol chain).

2.2.3.5 Synthesis of P2-24 latex

Styrene-copolymer latex with non-ionic emulsifier and cationic emulsifier, named P2-24, was prepared via four steps: 1-) Non-ionic emulsifier (1.37 g, 0.00065 mol), cationic emulsifier (1.37 g, 0.004 mol), the aqueous solution of ABVA (0.17 g, 10 mL DI water), and 22 mL DI water were poured in a beaker and stirred at 60°C. Afterward, styrene (17 g, 0.16 mol) was poured into the mixture, dropped wisely, and stirred for 30 minutes. 2-) Non-ionic emulsifier (1.37 g, 0.00065 mol) and cationic emulsifier (1.37 g, 0.004 mol) and 21 mL DI water were stirred in a beaker, then poured into a 250 mL three-necked round-bottom flask with a condenser and thermocouple and stirred at 300 rpm and at 75°C. The system was degassed for 30 minutes. 3-) The pre-emulsion was poured into an addition funnel and fed to the reaction mixture for 4 hours. The emulsion was stirred at 300 rpm 80°C. 4-) After the feeding, the reaction was stirred at 75°C for 2 hours. Post-procedure-The latex was filtered through a 300-mesh filter.

(Monomer conversion = 42.45%, $M_{n, \text{GPC}} = 4778000$ Da, $M_w/M_n = 1.2$).

$^1\text{H NMR}$ (CDCl_3 , δ): 7.10 (s, 2H, ArH, styrene), 7.05 (s, 3H, ArH, styrene), 6.58 (s, 2H, ArH, cationic emulsifier), 6.47 (s, 2H, ArH, cationic emulsifier), 3.66 (s, 171H, $\text{O}=\text{COCH}_2\text{CH}_2\text{OCH}_2\text{CH}_2\text{OCH}_2\text{CH}_2\text{OH}$, PEG chain), 2.70 (s, 1H, $\text{O}=\text{CHCH}=\text{O}$, maleic anhydride), 1.27 (m, 28H, $\text{O}=\text{COCH}_2\text{CH}_2\text{CH}_2\text{CH}_2$, alkyl chain of alcohol), 0.90 (s, 6H, $\text{NCH}_2\text{CH}_2\text{CH}_2\text{CH}_3$, terminal proton of alcohol chain).

2.2.3.6 Synthesis of P2-35 latex

Styrene-copolymer latex with non-ionic emulsifier and cationic emulsifier named P2-35 was prepared via four steps: 1-) Non-ionic emulsifier (2.30 g, 0.001 mol), cationic emulsifier (2.30 g, 0.007 mol), the aqueous solution of ABVA (0.17 g, 10 mL DI water), and 26 mL DI water were poured in a beaker and stirred at 60°C. Afterward, styrene (17g, 0.16 mol) was poured to the mixture, dropped wisely, and stirred for 30 minutes. 2-) Non-ionic emulsifier (2.30 g, 0.001 mol), cationic emulsifier (2.30 g, 0.007 mol), and 25 mL DI water were stirred in a beaker, then poured into a 250 mL three-necked round-bottom flask with a condenser and thermocouple, which was stirred at 300 rpm and at 75°C. The system was degassed for 30 minutes. 3-) The pre-emulsion was poured into an addition funnel and fed to the reaction mixture for 4 hours. The emulsion was stirred at 300 rpm 80°C. 4-) After the feeding, the reaction was stirred at 75°C for 2 hours. Post-procedure-The latex was filtered through a 300-mesh filter.

(Monomer conversion = 42.45%, $M_{n, GPC} = 10540000$ Da, $M_w/M_n = 1.1$).

$^1\text{H NMR}$ (CDCl_3 , δ): 7.10 (s, 2H, ArH, styrene), 7.04 (s, 3H, ArH, styrene), 6.58 (s, 2H, ArH, cationic emulsifier), 6.50 (s, 2H, ArH, cationic emulsifier), 3.66 (s, 171H, $\text{O}=\text{COCH}_2\text{CH}_2\text{OCH}_2\text{CH}_2\text{OCH}_2\text{CH}_2\text{OH}$, PEG chain), 2.76 (s, 1H, $\text{O}=\text{CHCH}=\text{O}$, maleic anhydride), 1.27 (m, 28H, $\text{O}=\text{COCH}_2\text{CH}_2\text{CH}_2\text{CH}_2$, alkyl chain of alcohol), 0.89 (s, 6H, $\text{NCH}_2\text{CH}_2\text{CH}_2\text{CH}_3$, terminal proton of alcohol chain).

2.3 Characterization of Non-ionic Emulsifier, Cationic Emulsifier, Latex, and Copolymer Film

2.3.1 Fourier Transform Infrared Spectroscopy(FTIR)

FTIR performed for analysis of structural properties of synthesized emulsifiers and copolymer films. (FTIR, Shimadzu- Infinity spectrometer, Japan) The analysis was performed with a range of $4000\text{-}500\text{ cm}^{-1}$ at room temperature with a resolution of 2 cm^{-1} and 64 scans. The detection of aromatic structure bonds, which were possessed by styrene monomers and cationic emulsifiers, and etheric bonds from

non-ionic emulsifiers were proof of the presence of the reactive emulsifiers within the polymer chain.

2.3.2 Scanning Electron Microscopy (SEM)

To investigate the morphology of dried PS film, the analysis was conducted with a current of 3-5 kV. (SEM LEO Supra 35 VP microscope, Germany) The copolymer latexes were drop-cast onto a silicon wafer. Subsequently, they were left to dry at 70°C for two days. To detect the film surface, gold/palladium coating was performed.

2.3.3 Thermal Gravimetric Analysis (TGA)

TGA was conducted to investigate the thermal stability of copolymer latex films and mass loss percentage versus temperature curve. Analysis was conducted between 25°C and 800°C by 10°C/min heating rate under a nitrogen atmosphere. (TGA instrument, Netsch)

2.3.4 Differential Scanning Calorimetry Analysis (DSC)

The copolymer latex films and emulsifiers thermal properties were analyzed by DSC between -30°C and 200°C with a heating rate of 5°C/min under a nitrogen environment. (TA Instruments – MDSCQ2000) T_g and T_m values were taken from the second heating cycle of the copolymer latex film samples.

2.3.5 Water Contact Angle Test

The hydrophilicity property of copolymer latex films was analyzed by contact angle shape analyzer. (Drop Shape Analyzer, KRUSS, Germany) The copolymer latex

films were dissolved in CHCl_2 and left to dry in a petri at 60°C for 1 day. The obtained films have an approximate width of 0.5 mm. By the Sessile drop method, 5 μL water was dropped onto films, and the water contact angle was calculated afterward. *P1-24, P2-24, and P2-35 were cast onto a glass plate by square frame, with an approximate width of 0.5 mm, and were left to dry at room temperature for two days.

2.3.6 Antibacterial Analysis

2.3.6.1 ASTM E2149 20 test

The antibacterial activity tests were conducted using Gram-positive bacteria (*Staphylococcus aureus* ATCC 6538) and Gram-negative bacteria (*Escherichia coli* ATCC 25922), respectively. We performed three duplicates of each test. We incubated the fresh bacterial cultures in Tryptic Soy Broth (Oxoid) 37°C prior to the tests. To achieve an absorbance of 0.28 ± 0.2 at 475 nm, corresponding to $1.5\text{--}3.0 \times 10^8$ CFU/mL, the bacterial suspensions were diluted with a clean 0.3 mM KHPO buffer solution. Then, the suspensions were further diluted until a final bacterial concentration of $1.5\text{--}3.0 \times 10^5$ CFU/mL was reached. 1 ± 0.1 g of granular material was introduced into sterile screw-cap flasks, and 50 ± 0.5 mL of the bacterial inoculum was added to each one. We incubated the flasks 37°C on a wrist-action shaker for 24 hours. We then extracted the samples from the flasks and neutralized them using polysorbate 80 and lecithin broth medium. We diluted the neutralized samples and plated them on Tryptic Soy Agar (Oxoid) three times for colony counting.

2.3.6.2 In-vitro ISO 22196 test

The antibacterial activity tests were conducted using Gram-positive bacteria (*Staphylococcus aureus* ATCC 6538) and Gram-negative bacteria (*Escherichia coli* ATCC 25922), respectively. Each test was conducted in triplicate. We propagated new bacterial cultures (18–24 hours old) in Tryptic Soy Broth (Oxoid) 37°C prior to tests. The bacterial suspensions were prepared in a sterile phosphate buffer and

adjusted by the turbidity method in accordance with McFarland Standard 1 over a 24-hour incubation period. The suspension was mixed with 1/500 Nutrient Broth (NB, Oxoid) until it reached a final concentration of $2.5\text{--}10 \times 10^5$ CFU/mL as the test standard. Then we used this as the test inoculum.

400 μL of inoculum was applied to each test piece (50×50 mm). To ensure complete contact between the bacterial suspension and the test sample, the suspension was covered with a sterile stretch film (40×40 mm). The test pieces were then incubated for 24 hours at 37°C under 90% relative humidity.

After the contact period, the samples were transferred into solution (Soybean Casein Lecithin Polysorbate 80 Medium, SCDLP Broth). After a 5-minute neutralization process, the samples were homogenized using a stomacher homogenizer to release the bacteria into the neutralizing solution.

2.3.7 Gel Permeation Chromatograph Analysis (GPC)

Molecular weight and polydispersity (PDI) values of copolymer latex films were determined with GPC analysis by a GPC instrument with a pump, refractive index, right-angle light scattering detector, low-angle light scattering detector, viscometer, and four PS-DVB columns (D5000, D3000) with reagent-grade DMF as a mobile phase within a 0.5 mL/min flow rate at 45°C . The effective molecular ranges of columns were 106 to 108 and 103 to 105 g/mol, respectively. (Viscotek GPCmax-VE 2001)

2.3.8 Nuclear Magnetic Resonance (NMR)

^1H (400 MHz) and ^{13}C (125 MHz) NMR spectra were recorded using an NMR instrument in CDCl_3 . (Varian UNITY INOVA)

2.3.9 Dynamic Light Scattering (DLS)

Particle size, PDI and Zeta-potential data of copolymer latex films were analyzed by a DLS instrument. (Zetasizer Nano—ZS, UK). The latexes were DI; the refractive index of copolymer latex is 1.59, and that of water is 1.30. Measurements were performed at room temperature, with three cycles per sample.

2.3.10 UV-VIS Spectroscopy (UV-vis)

The transmittance of copolymer latex films was determined by UV-vis instrument with 200-800 nm wavelength. (Shimadzu UV-3150 UV-VIS) The copolymer latex film was cast by square frame, with an approximate width of 0.5 mm, and was left to dry at room temperature for two days.

3. RESULTS AND DISCUSSION

3.1 Preparation of Non- Ionic Emulsifier

Ring-opening reaction between MA and 1-octadecanol and subsequent esterification reaction with PEG-2500 was performed according to the procedure that has been published. (Figure 3.1) (Solyman et al. (2018)).

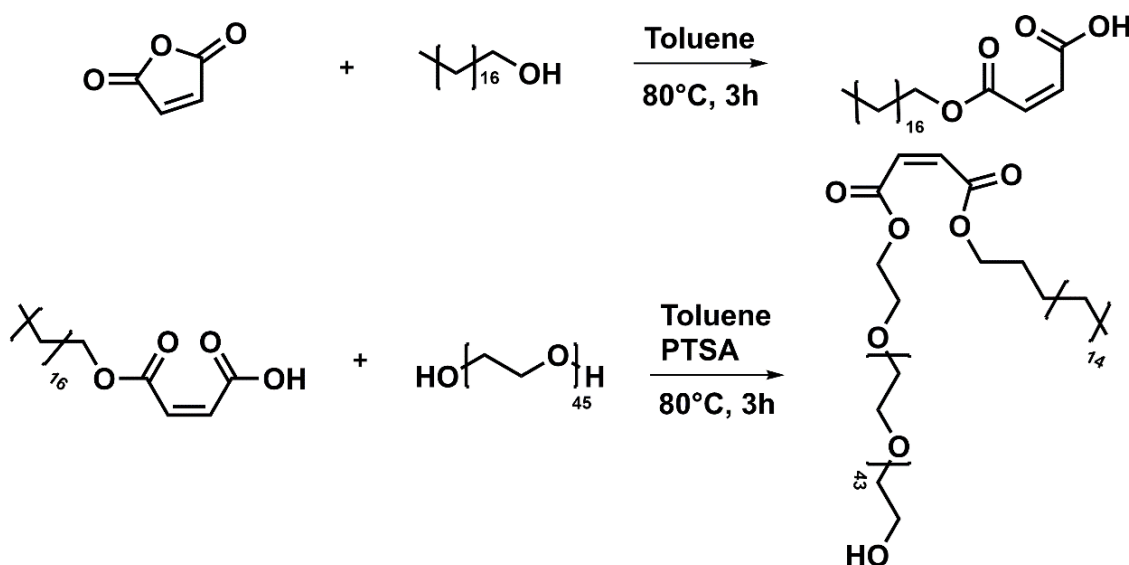


Figure 3.1 Schematic presentation of synthesis of non-ionic emulsifier.

From the ^1H NMR spectrum of the non-ionic surfactant, two protons of the double bond of the maleate group are found at 6.22 and 6.06 ppm, respectively. In addition, the etheric group, which is possessed by the PEG chain, is between 3.57 and 4.15 ppm, while the terminal group of alcohol is at 0.81 ppm. The mentioned signals confirm the protons and hence justify the molecule.

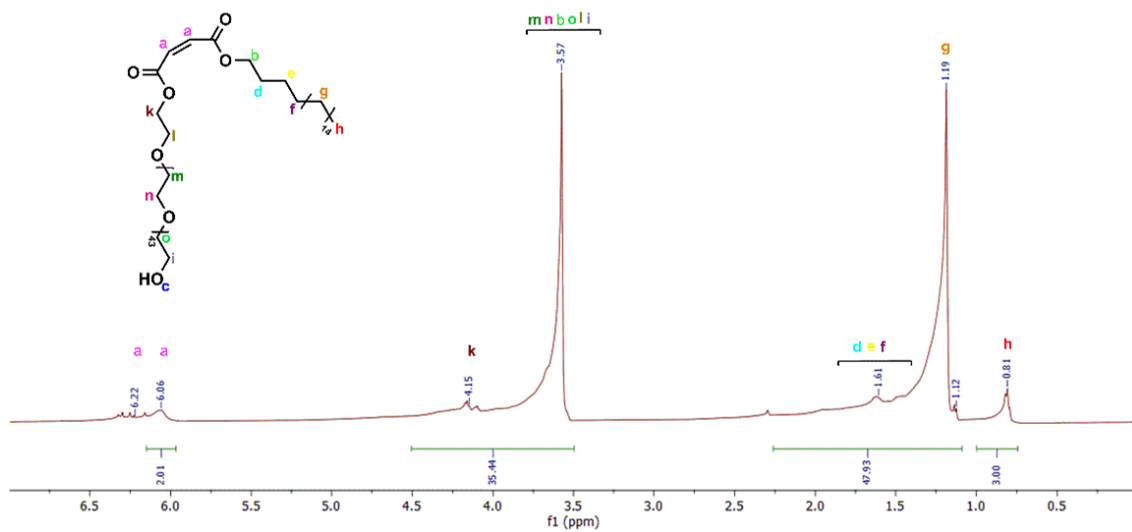


Figure 3.2 ^1H NMR spectrum of non-ionic emulsifier.

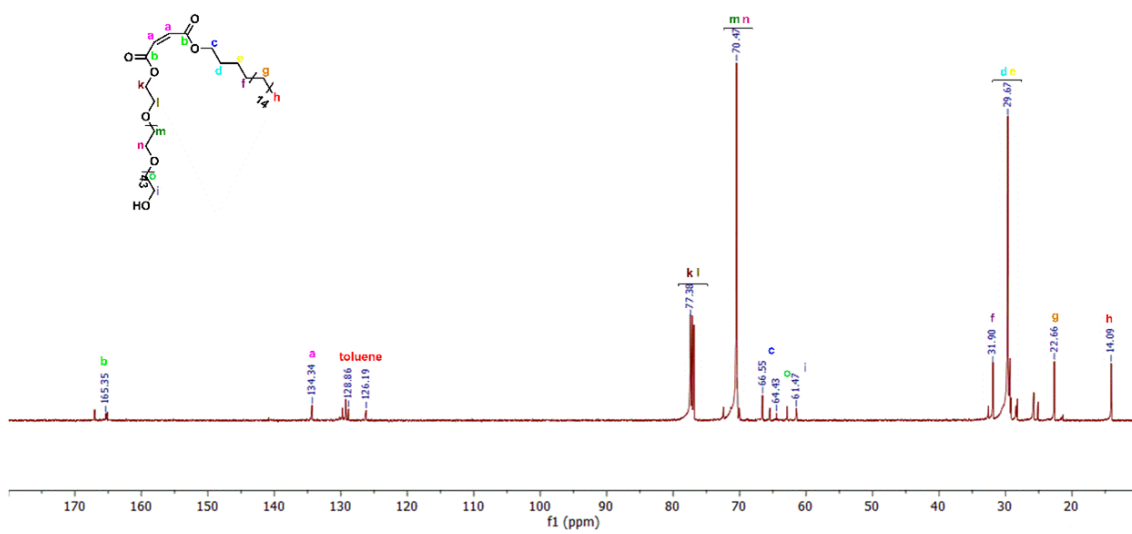


Figure 3.3 ^{13}C NMR spectrum of non-ionic emulsifier.

3.2 Preparation of Cationic Emulsifier

A cationic emulsifier was synthesized with vinyl benzyl chloride and N, N-dimethylcocoamine in a water (1:1) mixture, stirred at 75°C for 3 hours. The resulting product as yellowish viscous liquid.(Figure 3.4)

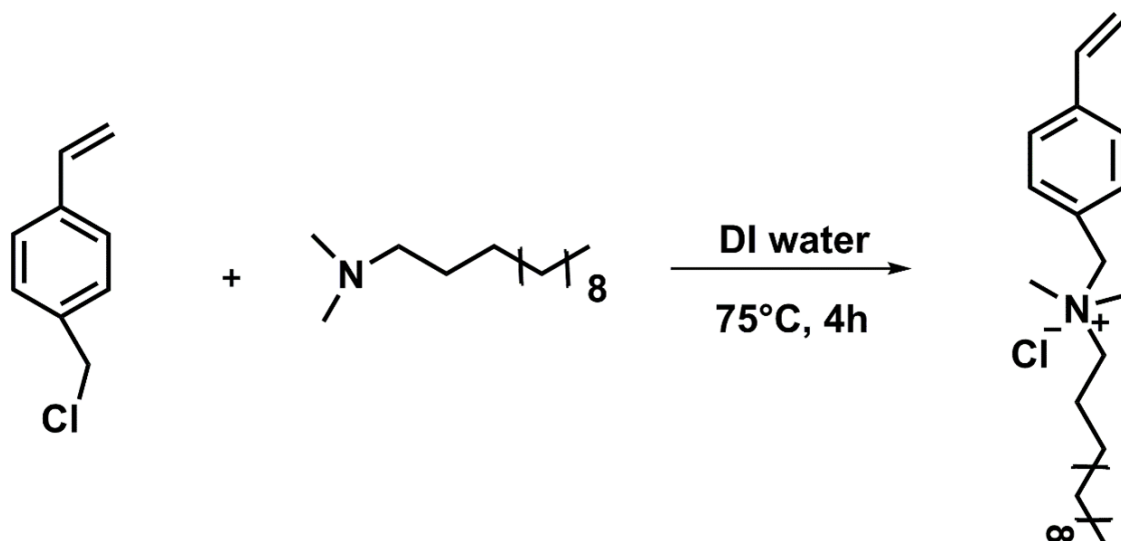


Figure 3.4 Schematic presentation of synthesis of cationic emulsifier.

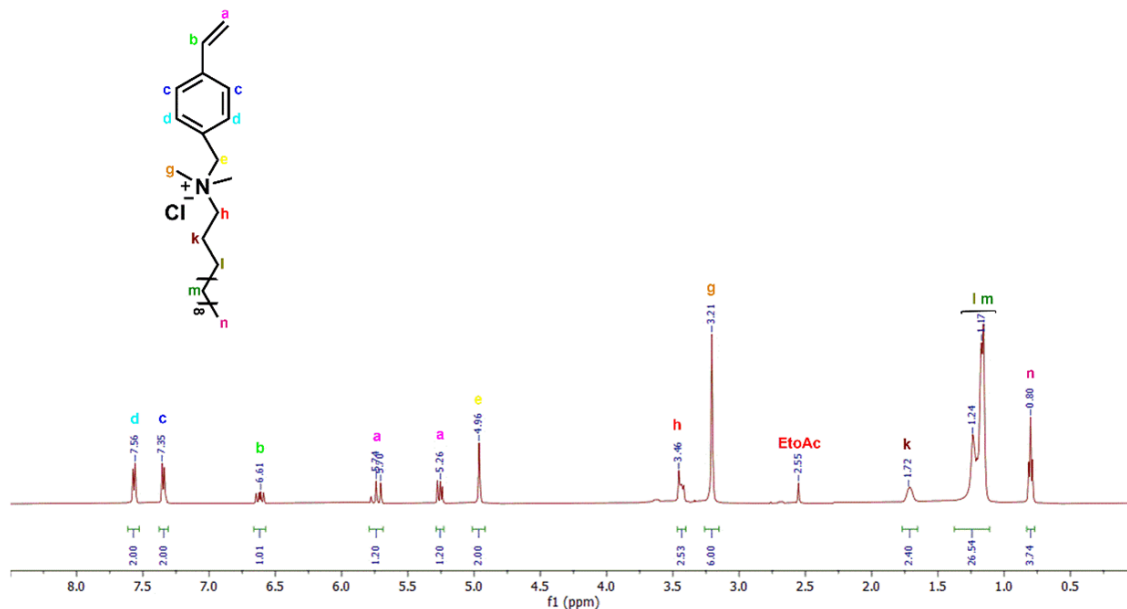


Figure 3.5 ¹H NMR spectrum of cationic emulsifier.

From confirm the number of protons on the molecule, justifying the ¹H NMR spectrum of cationic surfactant. Signals of the benzene ring were found at 7.56-7.35

ppm. In addition, two methyl groups of quaternized amine were found at 3.21 ppm, while protons between the benzene ring and quaternized amine were found at 4.96 ppm. The mentioned signals confirm the number of protons on the molecule and hence justify the molecule.

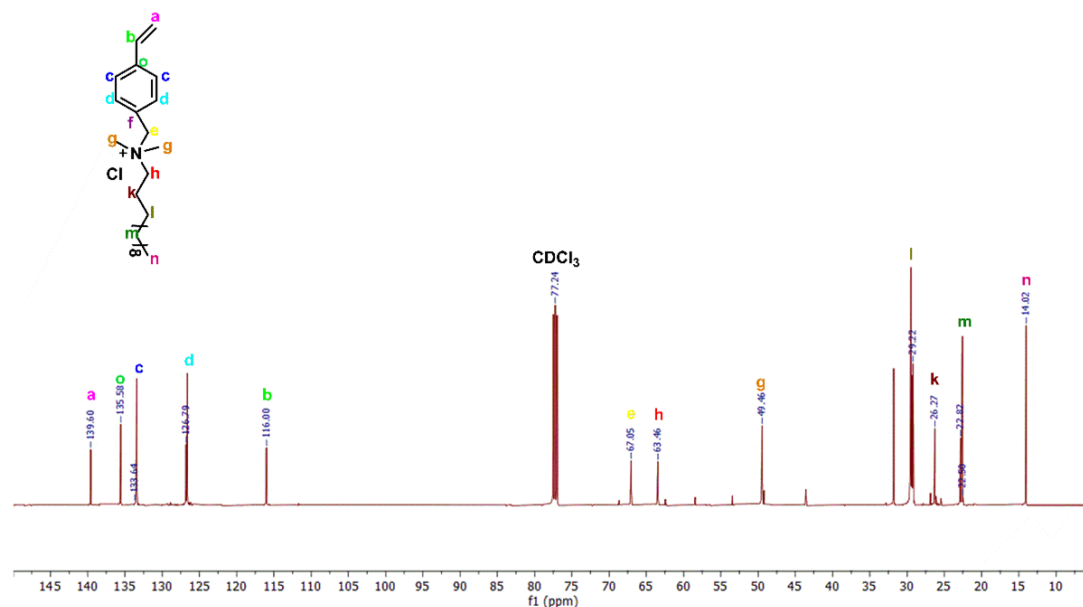


Figure 3.6 ^{13}C NMR spectrum of cationic emulsifier.

3.3 Preparation of Styrene Copolymer Latex Using Non-ionic and Cationic Emulsifiers

As given in Table 3.1, different weight ratios of reactive emulsifiers were formalized within the copolymerization of styrene, and a series of stable latexes were obtained. By mechanical stirring of styrene/reactive emulsifiers in the presence of a water-soluble initiator (APS, ABVA) at 80°C , stabilized latexes were observed. The weight percent of reactive emulsifiers was changed with the range of 19-35 wt.%, which was required to induce sufficient hydrophilicity. All copolymer latexes indicated high stability without phase separation and agglomeration, which were not observed during 30 days under room temperature conditions. The scope of the study is investigating antibacterial features, which will lead to good potential as a stable and antibacterial coating. The latexes and prepared polymer films were analyzed in detail with different characterizations.

Sample	Styrene	Non-ionic emulsifier	Cationic emulsifier	Initiator	DI water ^a
P1-19	0.16 mol - 17 g	0.0010 mol - 2.05 g	0.0062 mol - 2.05 g	0.17 g	49.27 g
P1-24	0.16 mol - 17 g	0.0013 mol - 2.74 g	0.0080 mol - 2.74 g	0.17 g	53.00 g
P1-35	0.16 mol - 17 g	0.0020 mol - 4.60 g	0.0140 mol - 4.60 g	0.17 g	61.13 g
P2-19	0.16 mol - 17 g	0.0010 mol - 2.05 g	0.0062 mol - 2.05 g	0.17 g	49.27 g
P2-24	0.16 mol - 17 g	0.0013 mol - 2.74 g	0.0080 mol - 2.74 g	0.17 g	53.00 g
P2-35	0.16 mol - 17 g	0.0020 mol - 4.60 g	0.0140 mol - 4.60 g	0.17 g	61.13 g

In emulsion polymerization of P1-19 to P1-35, APS was used as an initiator while ABVA was used for P2-19 to P2-35.

^a*Solid content of emulsions were 30 wt. %.*

Table 3.1 The weight ratio of styrene, copolymer latexes, by using reactive non-ionic emulsifiers and cationic emulsifier.

According to Table 3.2, six different experiments were conducted using three distinct feeding ratios of reactive emulsifiers, categorized under two types of initiators. The content of reactive emulsifiers ranged from 19 to 35 wt. %.

The emulsions were prepared in a four-necked round-bottom flask containing distilled water and half the total weight of emulsifiers. The flask was equipped with a condenser, thermocouple, and two additional funnels for feeding. A pre-emulsion was prepared by dissolving half the weight of the surfactant in distilled water, followed by the dropwise addition of styrene. The mixture was stirred thoroughly to ensure the formation of a stable emulsion.

Before feeding the initiator and pre-emulsion, the system was degassed for 30 minutes at 80°C. Due to solubility issues with APS (unlike ABVA, which showed no such problems), separate feedings were employed. The feeding process lasted 4 hours, with both feeds introduced at a controlled rate to prevent rapid polymerization. After the feeding phase, stirring continued.

Sample	Feed monomer content (mol%)	Feed emulsifier content (wt%)	Initiator	Monomer conversion (%) ^a	Solid content (wt%) ^a
P1-19	0.16	19	APS	42.45	12.73
P1-24	0.16	24	APS	35.00	10.33
P1-35	0.16	35	APS	40.20	12.04
P2-19	0.16	19	ABVA	95.00	28.38
P2-24	0.16	24	ABVA	99.00	29.80
P2-35	0.16	35	ABVA	66.00	20.24

^aDetermined gravimetrically.

Table 3.2 Optimization of styrene, copolymer latexes by using reactive non-ionic emulsifiers and cationic emulsifier.

The final emulsion was filtered by 300-mesh filter to remove aggregated polymers. Across all six experiments, external parameters such as dosage rate, reaction time, temperature, stirring speed, and duration were kept constant. The targeted theoretical solid content for all runs was maintained at 30 wt.%.

Sample	Emulsifiers content in copolymer (%) ^a	M_n (Da) ^b	PDI (M_w/M_n)
P1-19	55/1/44	10950000	1.78
P1-24	53/7/39	2080000	1.45
P1-35	52/2/4	1796000	1.30
P2-19	53/1/46	45450000	1.22
P2-24	55/1/44	4778000	1.16
P2-35	54/2/44	10540000	1.10

^aThe efficiency of the formation of styrene/non-ionic emulsifier/cationic emulsifier was determined by ¹H NMR.

^b GPC analysis was done relative to LC standards.

Table 3.3 Efficiency of copolymer latex film sty/non-ionic emulsifier/cationic emulsifier and molecular weight values.

The ^1H and ^{13}C NMR spectrums provided valuable information for calculating the efficiency and the structure of copolymers in the latex films. General fashion for all the copolymer latex films, the ^1H NMR spectra exhibited shifts in the signals of aromatic protons of the cationic emulsifier around 6.50 and 6.40 ppm, respectively, due to the resonance effect of the PEG chain Barboiu, Streba, Luca, Radu & Grigoriu (1998). Additionally, a characteristic signal at 3.66 ppm was assigned to the PEG moiety in figure 3.7. The aliphatic protons of the alcohol chain and the alky chain of the cationic emulsifier were found between 1.5 and 0.80 ppm in conjunction with the protons of the main polymer chain. The methine proton of styrene appeared around 2.74-2.76 ppm. Furthermore, GPC traces of the copolymer latex films revealed a correlation between monomer conversion and molar mass, with narrow dispersity in the range of 1.1-1.78. As the amount of emulsifier increased, the molar mass increased proportionally, consistent with the monomer conversion values. (Table 3.3) However, another aspect related to molecular weight is that smaller particle sizes tend to decrease the interfacial area of the latex, consequently decreasing molecular weight. Another factor influencing molecular weight is the emulsifier used, as higher emulsifier content leads to rapid polymerization, forming low molecular weight particles Sardari & Mannari (2024).

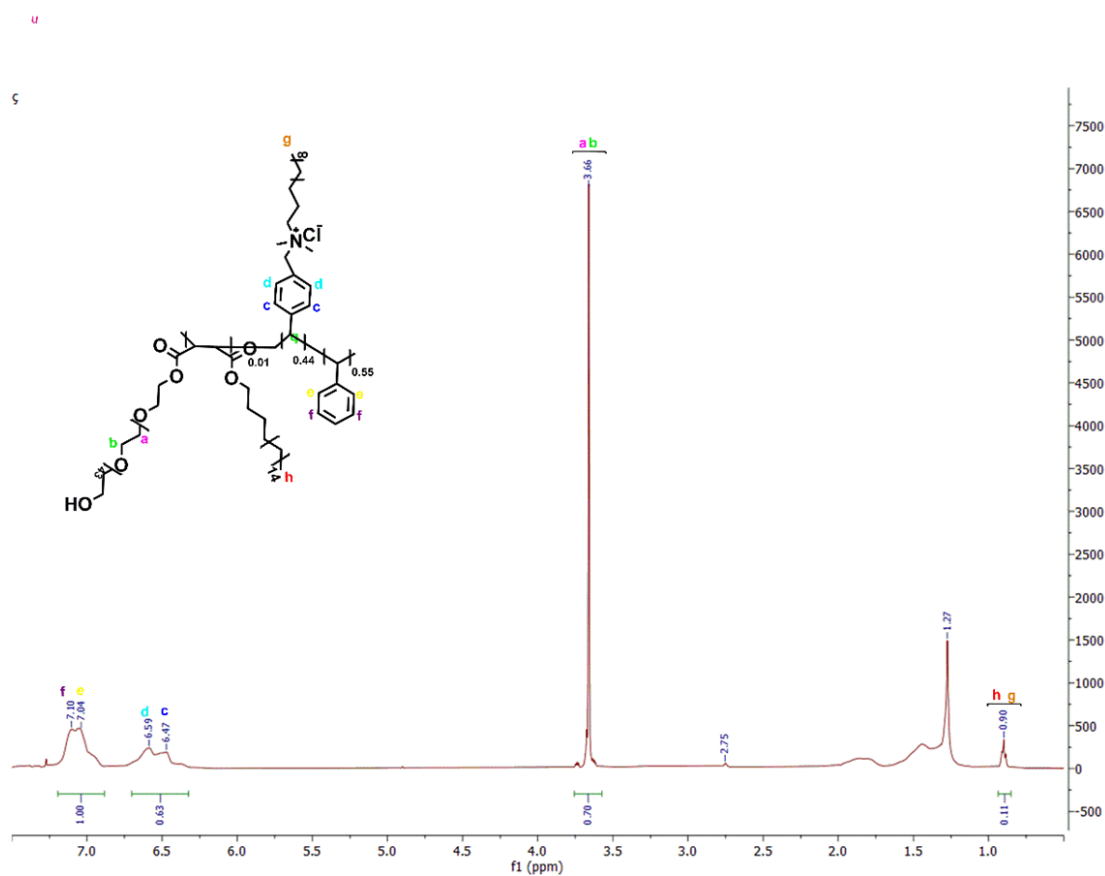


Figure 3.7 ^1H NMR spectrum of P1-19.

c

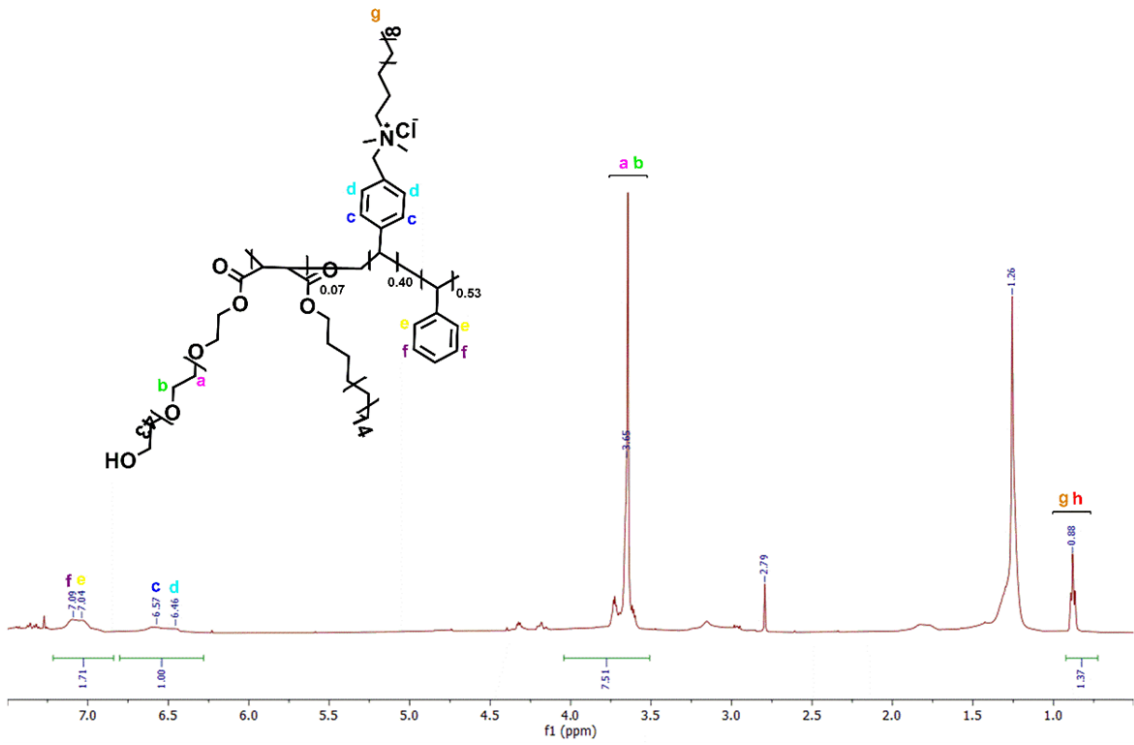


Figure 3.8 ¹H NMR spectrum of P1-24.

c

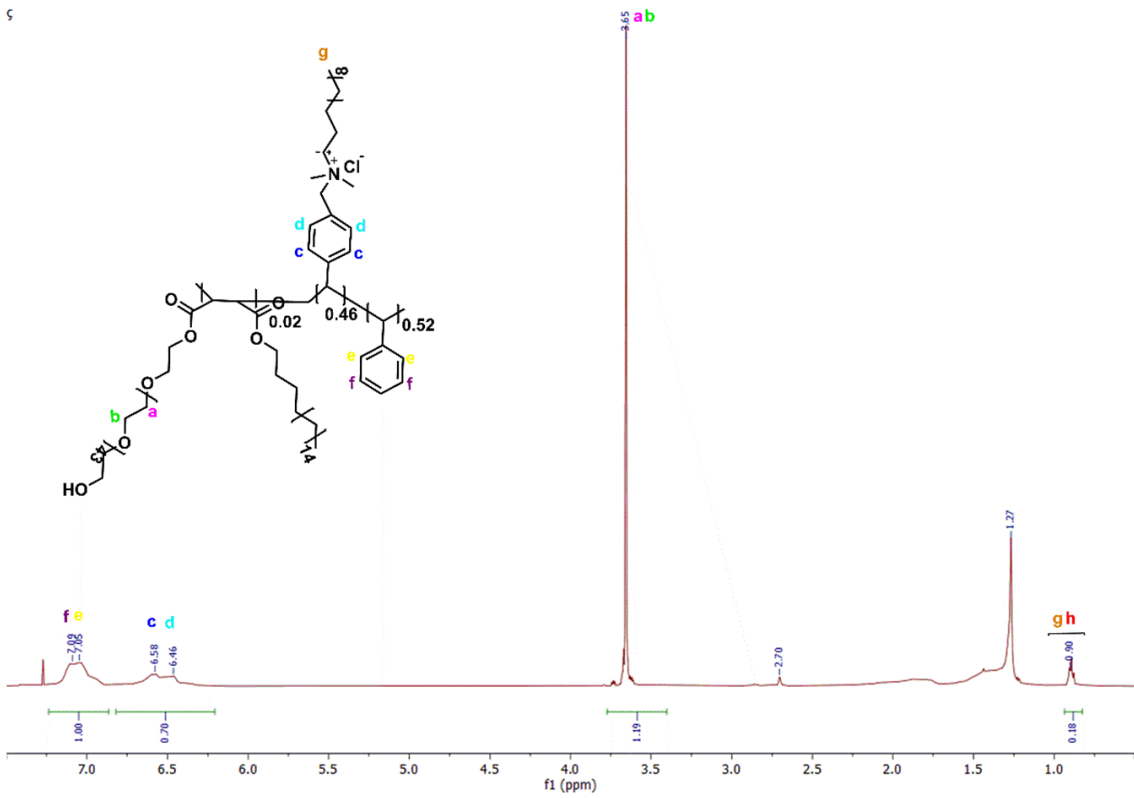


Figure 3.9 ¹H NMR spectrum of P1-35.

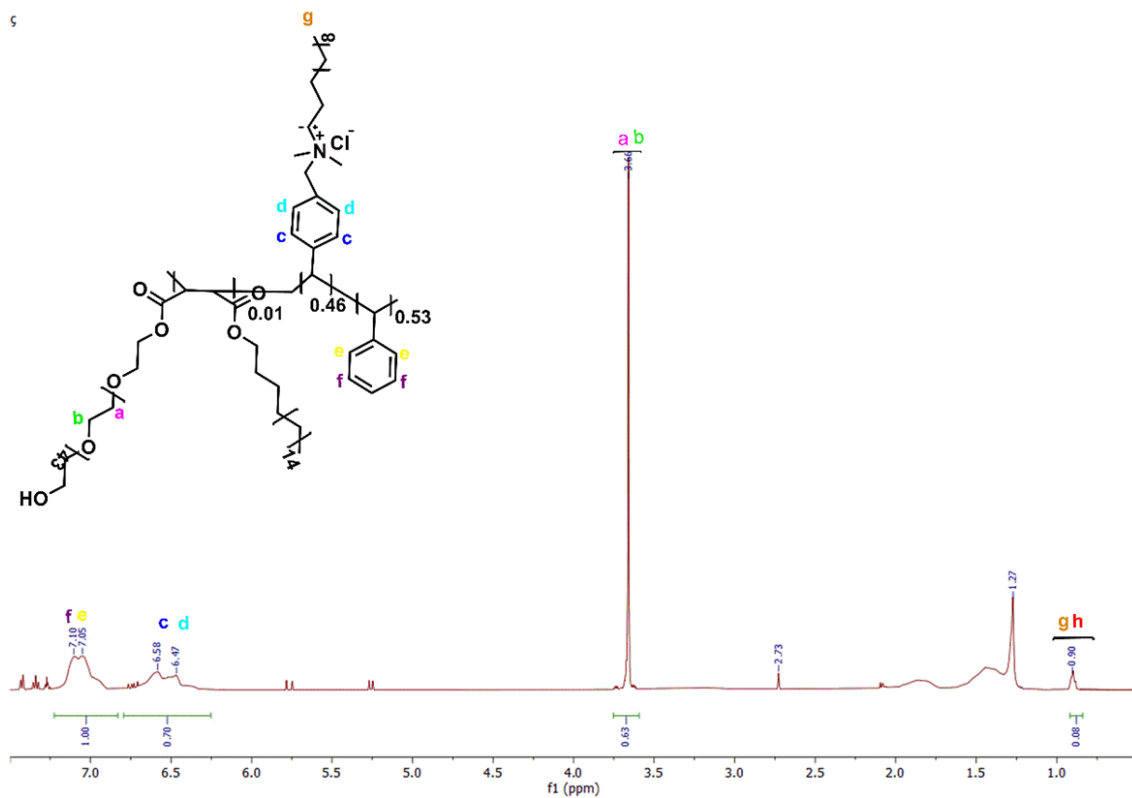


Figure 3.10 ^1H NMR spectrum of P2-19.

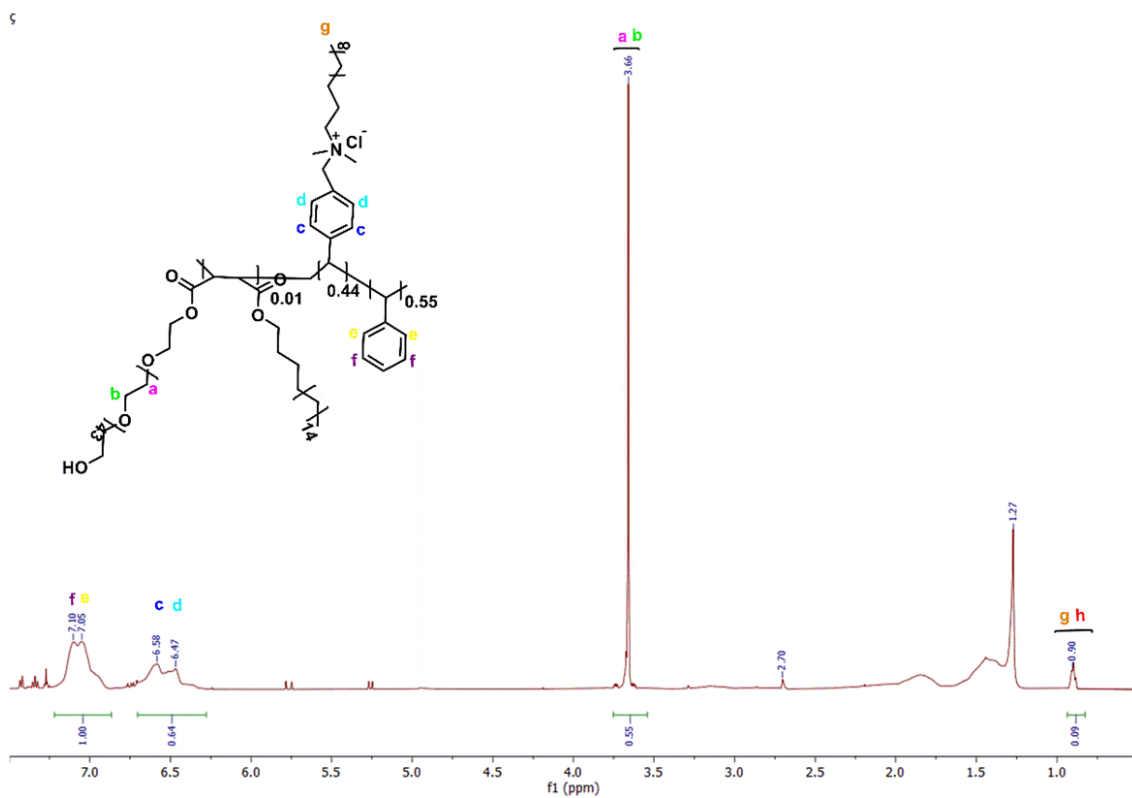


Figure 3.11 ^1H NMR spectrum of P2-24.

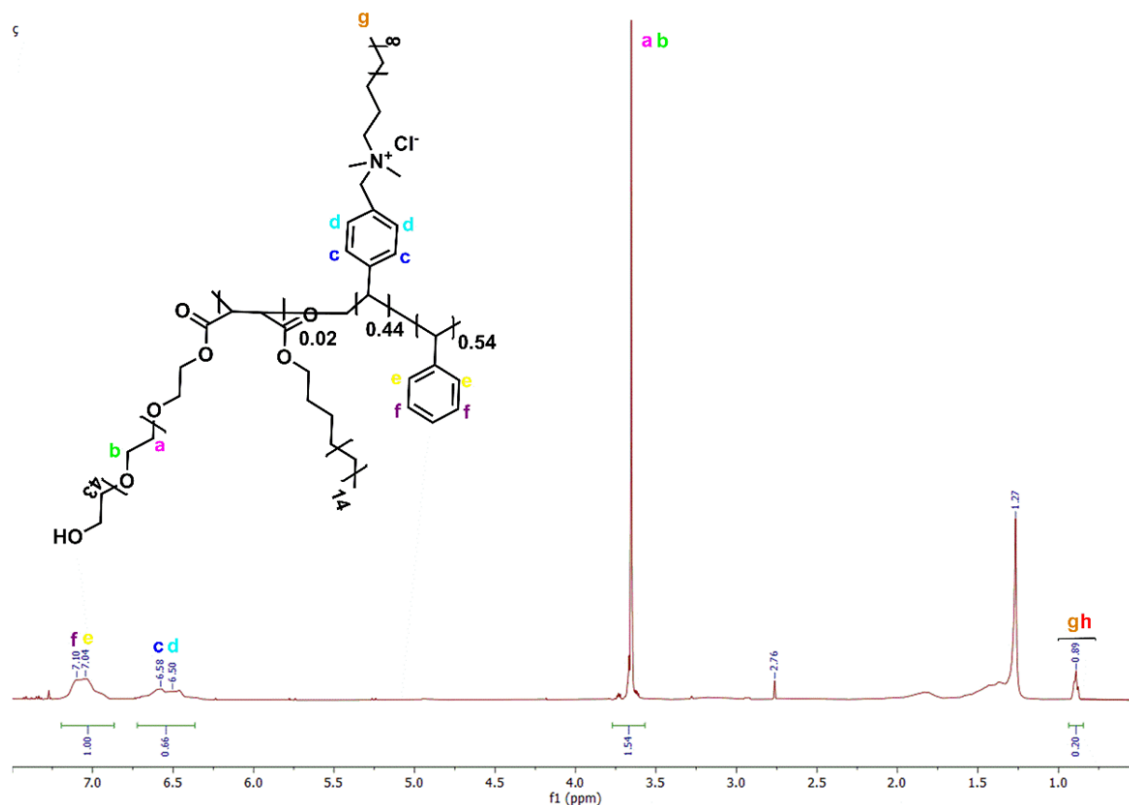


Figure 3.12 ¹H NMR spectrum of P2-35.

3.4 FTIR Analysis

FTIR spectra of copolymer latex films and emulsifiers were recorded to examine the chemical structure of polymer chains, as shown in Figures 3.13 and 3.14. The characteristic peaks of the cationic emulsifier include a broad peak at 3395 cm^{-1} , which corresponds to N-H stretching, is disappeared as expected. Additionally, peaks at 2922 cm^{-1} and 2853 cm^{-1} are attributed to the alkyl group's symmetric and asymmetric C-H₂ stretching vibration. Other significant peaks observed include a band at 1456 cm^{-1} , associated with CH₂ stretching vibrations in the alkyl chain and the CH bonding in methyl and methylene groups, respectively (Yue, Zhang, Li, Su, Jin & Qin (2019)). A peak at 740 cm^{-1} corresponds to double carbon bond stretching vibration and bending vibrations. A distinctive peak of non-ionic emulsifier at 1110 cm^{-1} corresponds to stretching vibrations of the CH₂ group in the PEG moiety. The characteristic peak for maleic anhydride, associated with tensile vibration of the carbonyl group, appeared at 1710 cm^{-1} .

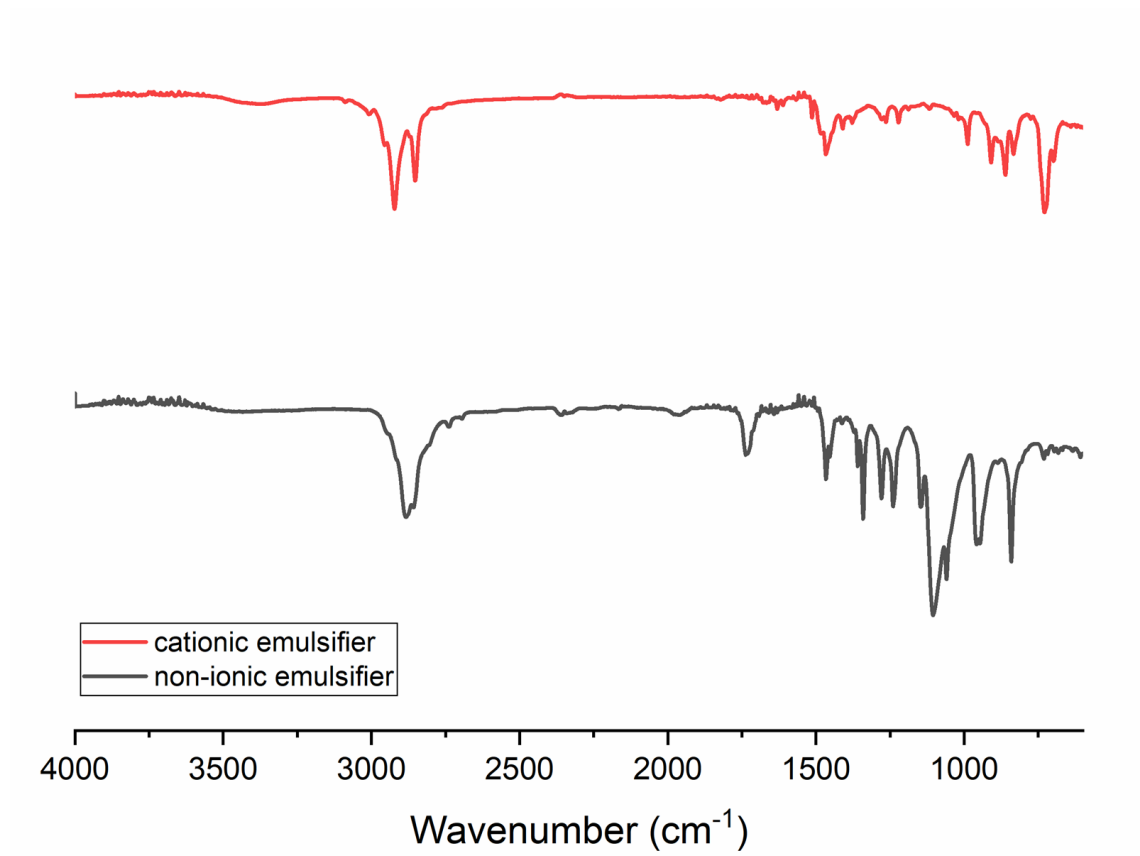


Figure 3.13 FTIR spectra of non-ionic emulsifiers and cationic emulsifiers.

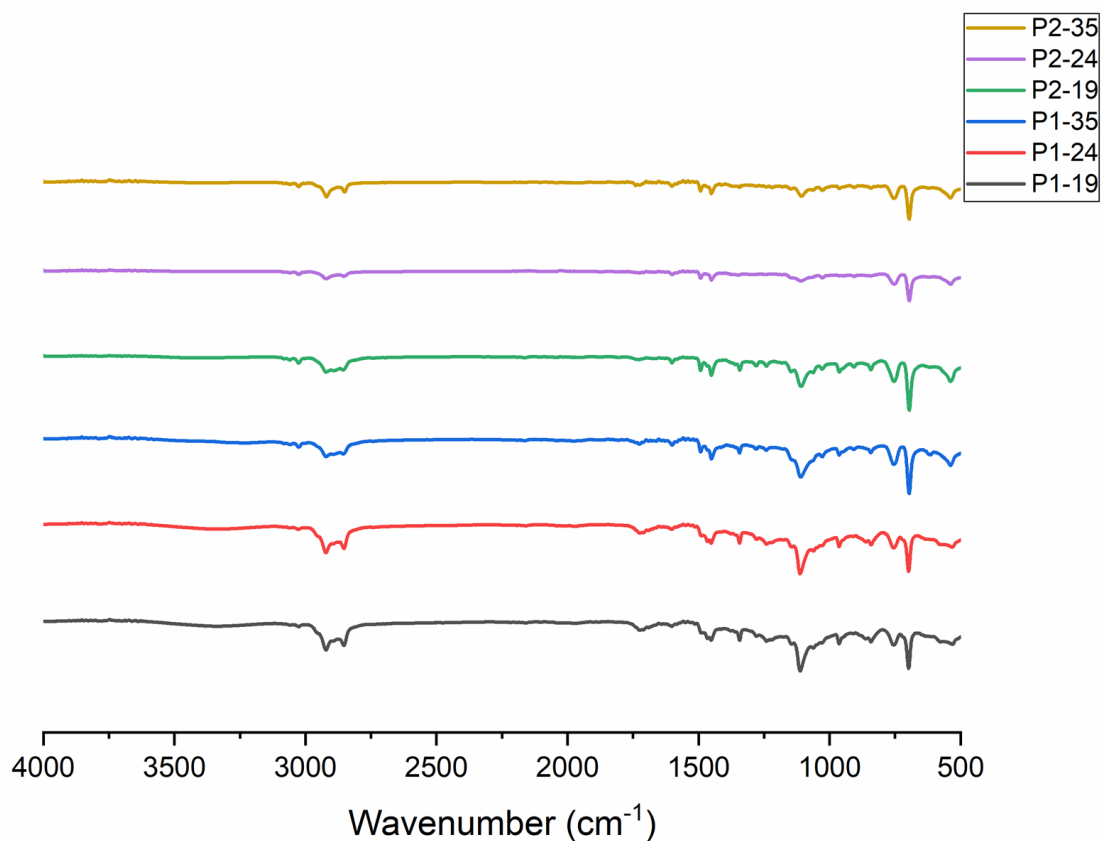


Figure 3.14 FTIR spectra of copolymer latex films.

The chemical structure of copolymer latex films chains is represented in Figure 3.14. The asymmetric and symmetric stretching and vibrations of CH_2 are attributed to the elimination of double bonds of styrene and both reactive emulsifiers, which is a key method for monitoring the polymerization reaction. Since all polymer films bear an aromatic structure, the peak at 1455 cm^{-1} corresponds bending vibrations of the CH_2 and benzene ring. The broadband between $1728\text{--}1730\text{ cm}^{-1}$ is due to the carbonyl group of the nonionic emulsifier, while the band at around 1100 cm^{-1} indicates the ethereal bond C-O-C bond of PEG moiety in the non-ionic emulsifier. The disappearance of a double bond around 1637 cm^{-1} indicates the occurrence of polymerization.

Since all copolymer latex films contain ester and carbonyl groups, a weak stretching band of ester group C=O is observed around 1100 cm^{-1} , further confirming that polymerization has occurred. These stretching bands provide clear evidence of the chemical changes that occurred during polymerization and serve as a valuable tool for monitoring the progress of the reaction.

3.5 Morphological Characterization of the Copolymer Latex Films

Surface chemistry plays a significant role in the arrangement of the surface. The surface morphology of copolymer latex films, composed of varying weight ratios of non-ionic and cationic emulsifiers with styrene, was investigated using SEM. All samples exhibited relatively even surfaces, although some particles were observed to have aggregated in certain cases. To understand the behavior of films, it is essential to comprehend the film formation process. By evaporation of water, the particles encounter each other and, subsequently, form a void-free, transparent film. In a binary latex system, the hard particles cannot deform; therefore, soft particles are chosen binders. As shown in Figure 3.15, a non-ionic emulsifier acts as a soft segment due to the PEG moiety, while a bulky aromatic ring and long alkyl chain functions as hard segments in a latex system (Feng, Winnik, Shivers & Clubb (1995), Steward, Hearn & Wilkinson (2000)).

As mentioned, all SEM micrographs show an even surface. As the efficiency of the non-ionic emulsifier increases, the particle size decreases, leading to a more uniform surface without cracks or coalescence.

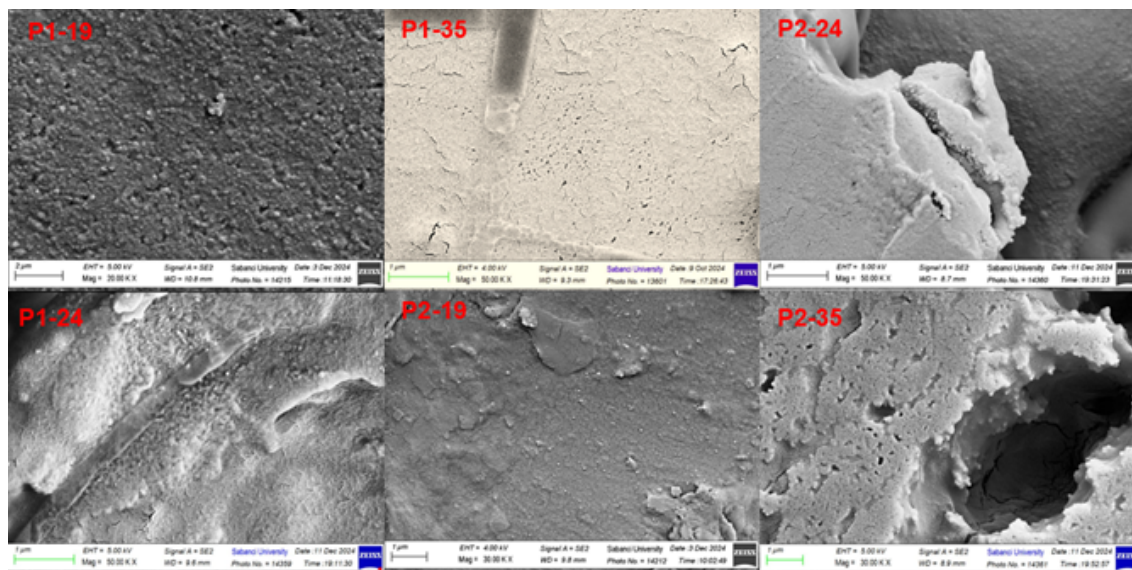


Figure 3.15 SEM micrographs of copolymer latex films.

3.6 Transparency Analysis of Copolymer Latex Films

The copolymer latex films exhibited high optical transparency, as indicated by their transmittance of % in UV-Vis spectra. The degree of opacity in films depends on factors such as void concentration, particle size, and distribution. The addition of a non-ionic emulsifier to the latex system was found to increase coalescence while reducing particle flocculation during film formation, leading to defect-free films. While P1-19 displays lower efficiency of the non-ionic emulsifier on the polymer chain, it exhibits lower transparency.

As previously mentioned, the efficiency of ionic emulsifiers plays a significant role in transparent films. Although the amount of emulsifier is important, P2-35 (Figure 3.16) shows lower transmittance due to depletion flocculation. Specifically, the development of micelles at high emulsifier concentration induces osmotic pressure, which causes particle flocculation (Feng et al. (1995)). This phenomenon negatively affects the transparency of films.

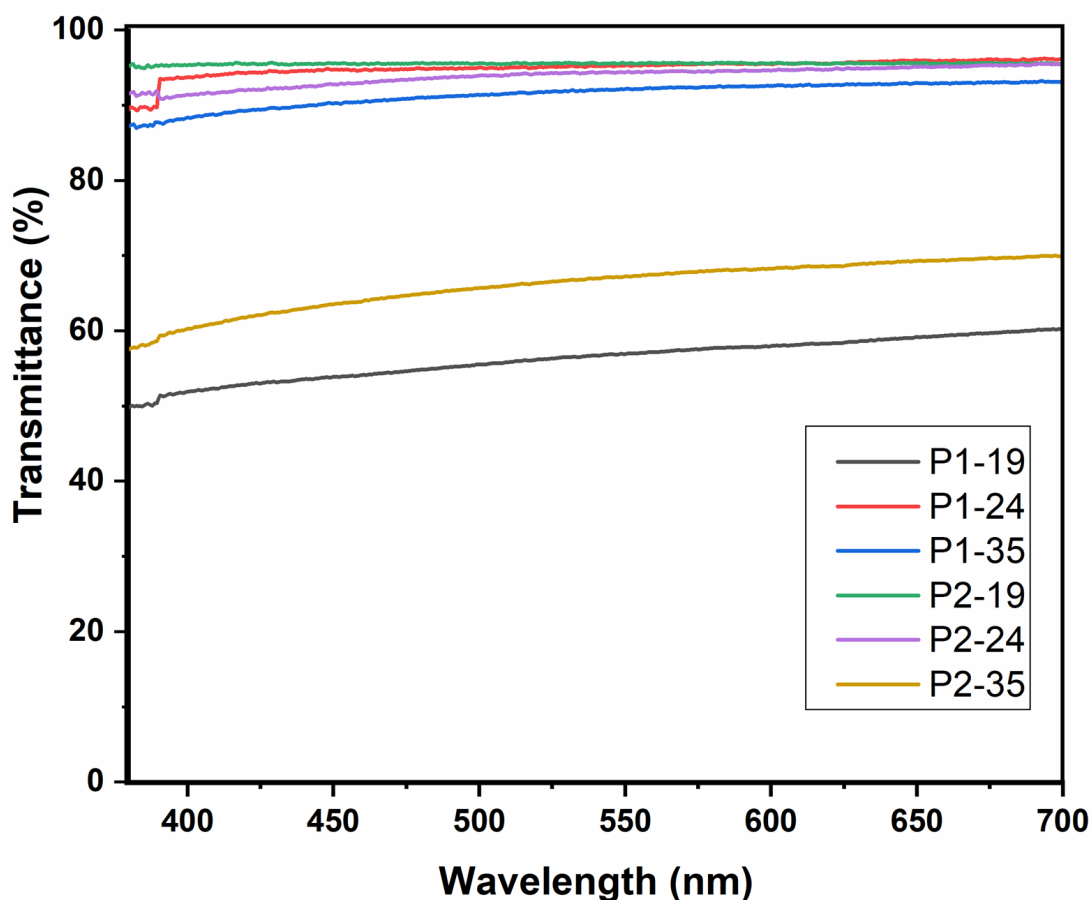


Figure 3.16 Transmittance values of copolymer latex films.

3.7 Contact Angle Measurements

Contact angle analysis is an adequate technique to determine the hydrophobicity or hydrophilicity of polymer surfaces; a contact angle higher than 90° indicates hydrophobicity, whilst a contact angle below 90° denotes hydrophilicity (Feng et al. (1995), Steward et al. (2000)). The desorption energy of the particles is closely linked to their hydrophobicity, highlighting the critical role of the surfactant composition in controlling surface behavior plays a significant role.

Contact angles of copolymer latex films provide valuable understanding of the surface hydrophilicity and hydrophobicity of the copolymer films with varying emulsifier ratios and efficiencies. As presented data in Figure 3.17, it was observed that the contact angles of the samples vary depending on the emulsifier composition; more specifically, the non-ionic emulsifier containing a long PEG chain contributes significantly to the hydrophilic nature of the copolymer films. For instance, the contact angles of P1-19 ($66.06^\circ \pm 5.37^\circ$) and P1-24 ($54.65^\circ \pm 5.03^\circ$) suggested moderately hydrophilic surfaces, primarily influenced by the non-ionic emulsifier content, which promotes water permeability.

Despite the emulsifier ratio of P2-19 ($101.32^\circ \pm 1.30^\circ$) and P2-24 ($72.08^\circ \pm 12.29^\circ$), they showed higher contact angles, which can be attributed to the increased efficiency of styrene and cationic emulsifiers ratio on the polymer chain. The bulky benzene group of the styrene and long alkyl chain of cationic emulsifier are known to reduce the hydrophilicity of the surface, leading to more hydrophobic behavior. The significant difference between P1-19 and P2-19 further emphasizes the role of the emulsifier ratio, where a higher amount of cationic emulsifier increases the hydrophobicity, as observed in the contact angle shift from 66.06° to 101.32° .

Moreover, the contact angle values for P1-35 ($75.79^\circ \pm 6.58^\circ$) and P2-35 ($57.08^\circ \pm 1.30^\circ$) provide additional evidence that copolymer efficiency on polymer chain plays a crucial role in determining the surface characteristics. P1-35, with a higher efficiency of the styrene and cationic emulsifier, exhibits a more hydrophobic surface (75.79°). In contrast, P2-35, which contains a higher efficiency of the non-ionic emulsifier, indicates more hydrophilic properties with a contact angle of 57.08° .

An increase in non-ionic emulsifier efficiency in a polymer chain tends to decrease the contact angle and shift towards hydrophilic behavior. In contrast, the higher efficiency of styrene and cationic emulsifiers, with their bulky hydrophobic groups, leads to an increase in the contact angle, indicating hydrophobicity.

The particles' desorption energy is closely linked to their hydrophobicity, as quantified by the contact angle, highlighting the critical role of the surfactant composition in controlling surface behavior.

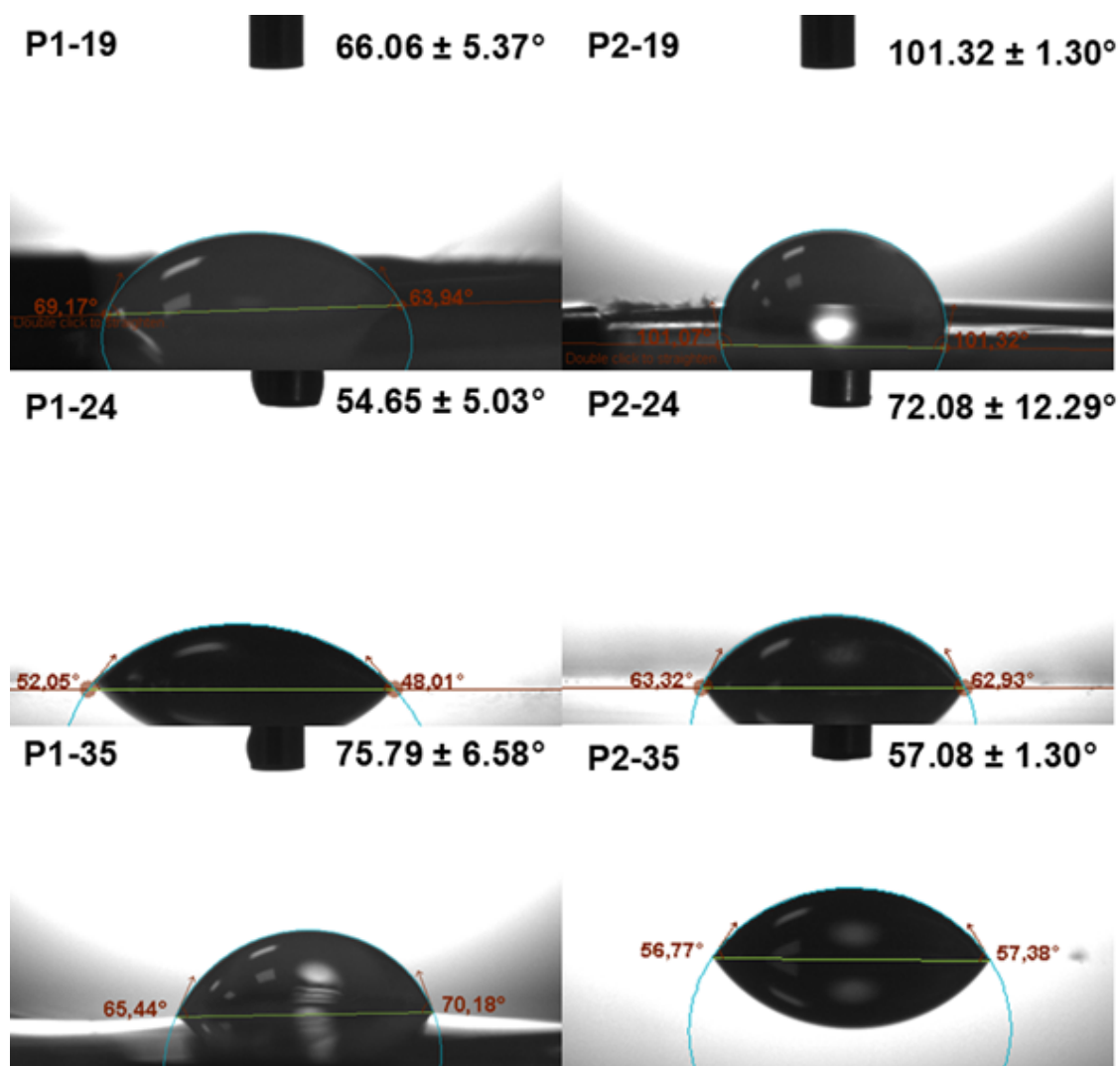


Figure 3.17 Contact angle of copolymer latex films of P1-19, P1-24, P1-35, P2-19, P2-24, P2-35.

3.8 The Dynamic Light Scattering Analysis of Copolymer Latexes

An analysis of the six copolymer latexes presented in table 3.4 with their particle size, zeta potential, and PDI values. The latexes were studied on both the 0th day and after 30 days to assess their stability.

Sample	Particle Size (nm) ^a		PDI ^b		Zeta Potential (mV) ^c
	0 th Day	30 Days	0 th Day	30 Days	
P1-19	237.2	238.00	0.092	0.133	17.10
P1-24	316.3	220.30	0.241	0.200	17.40
P1-35	237.2	278.00	0.092	0.259	15.80
P2-19	159.8	189.00	0.207	0.230	46.10
P2-24	97.0	90.26	0.093	0.073	36.90
P2-35	129.3	106.50	0.347	0.231	17.98

^aParticle size distribution of 0th day storage and 30 days storage.

^bParticle size distribution of 0th day storage and 30 days storage.

^cAverage zeta-potential values of 0th day storage and 30 days storage.

Table 3.4 Particle size distribution profiles 0th days, 30 days of storage.



Figure 3.18 P1-19, P1-24, P1-35, P2-19, P2-24, and P2-35 emulsions on day 30.

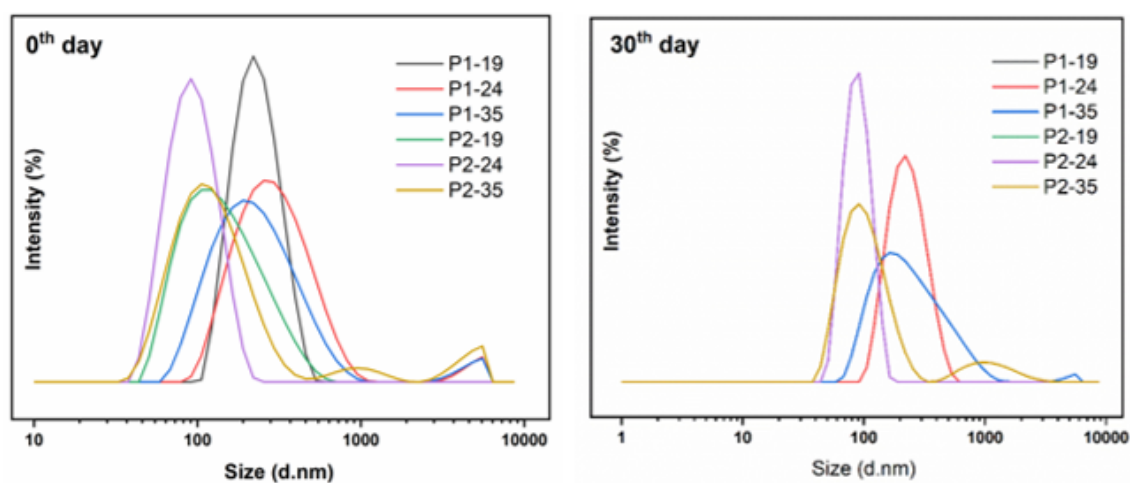


Figure 3.19 DLS analysis of 0th day, 30 days of storage.

The particle size, zeta potential, and particle size distribution values play significant roles in the properties and performance of latexes (Clogston & Patri (2011)). The PDI values range from 0.1 to 0.25, displaying enhanced system stability; thus, lower PDI values result in increased system stability.

On the 0th day, as shown in Figure 3.18, the particle sizes varied from 316 nm to 97 nm across the samples. The particle size distributions were narrow from 100 nm to 900 nm, and the PDI value was between 0.09 and 0.02, which is a significant indicator of good dispersion and stability for P1-19, P2-19, and P2-24, while P1-24, P1-35, and P2-35 spread a bimodal distribution with a PDI value between 0.09 and 0.3.

The emulsifier concentration affects the particle size and, apparently, the number of particles. At high emulsifier concentrations, all monomers are dwelled within micelles, correspondingly generating particles a size of less than 100 nm. For instance, P2-24. Further, as it has been mentioned previously, reduction in emulsifier concentration will increase the tendency of the generation of larger particles. Consequently, extensive coagulation of the initial particles takes place, and the creation of large particle sizes, for instance, P1-19, P2-19 (Clogston & Patri (2011)).

After 30 days, there were only slight drops in the particle sizes without any phase separation, which suggests that the latexes maintained their stability. The PDI values, which reflect the uniformity of the particle sizes within each sample, showed minimal change over 30 days, although the particle size distribution became more uniform over time. Stability of latexes is evaluated by their zeta potential values. The electrostatic stability of particles for cationic and anionic systems is accepted as greater than +30 mV or less than -30 mV, respectively. The changes on the surface of the particle imply a function of zeta potential (Sun, Yuan, Zhang, Cao & Sun (2017)).

The zeta potential remained relatively stable after 30 days. P2-19 had the highest zeta potential at 46.1 mV on the 0th day, indicating excellent stability. Other latexes showed zeta potentials ranging from 15.8 mV to 36.9 mV on the 0th day. These high zeta potential values suggest that the latexes are well-dispersed and resistant to aggregation, ensuring good colloidal stability.

The tendency to form hydrogen bonds of comonomers in the polymer chain affects the hydrophilicity of the polymer chain and, apparently, the zeta potential [20]. Attributed to the polar nature of hydrophilic groups, polar interactions will result in an increment of zeta potential value, for instance, P2-24.

The particle size remained relatively consistent, and the high zeta potential values

confirmed their stability. This suggests that these latex formulations are well-suited for applications where long-term stability is crucial, with little risk of aggregation or instability.

3.9 Antibacterial Test Analysis

Represented ASTM 2149 test results, P1-19, P2-24, and P2-19 compounds exhibited antibacterial activity against both Gram-positive and Gram-negative bacteria by providing >99.9999% (> 6 logs) at 24-hour contact time. Despite the results, P2-35, which indicated the least antibacterial effect, also exhibited strong antibacterial activity with > 3 log decrease (> 99.98% mortality) against two representative bacteria. Table 3.5 and Table 3.6 show the results of synthesized compounds against Gram-positive and Gram-negative, respectively.

Sample	Number of cells (cfu/ml) ^a	Reduction (%)
P1-19	< 30*	> 99.99998
P2-19	1.32×10^5	> 99.93400
P2-24	< 30*	> 99.99998
P2-35	< 30*	> 99.99998
Control	3.20×10^8 (0.h)	2.00×10^8

Table 3.5 Antibacterial test of copolymer latexes towards Gram-positive bacteria (*S. aureus* ATCC 65) by ASTM E2149 standard method.

^aThe less than 30 cfu/ml count as 30.

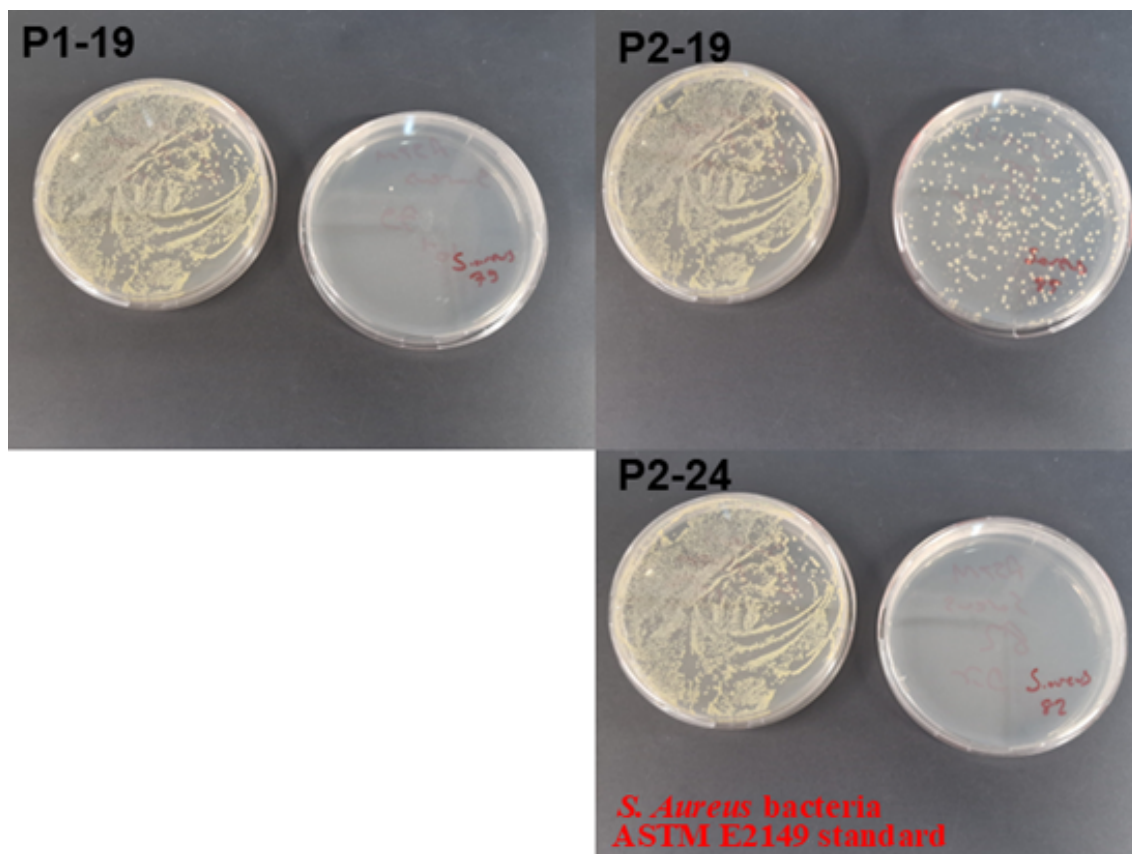


Figure 3.20 The right sample, coated with copolymer latexes, and the left control were assessed for their antibacterial efficacy of Gram positive bacteria by ASTM E2149 standard method.

Sample	Number of cells (cfu/ml)	Reduction (%)
P1-19	< 30*	> 99.99998
P2-19	5.7×10^4	> 99.96400
P2-24	< 30*	> 99.99998
P2-35	< 30*	> 99.99998
Control	1.70×10^5 (0.h)	1.60×10^8

Table 3.6 Antibacterial test of copolymer latexes towards Gram negative bacteria (*E. coli* ATCC 2592) by ASTM E2149 standard method.

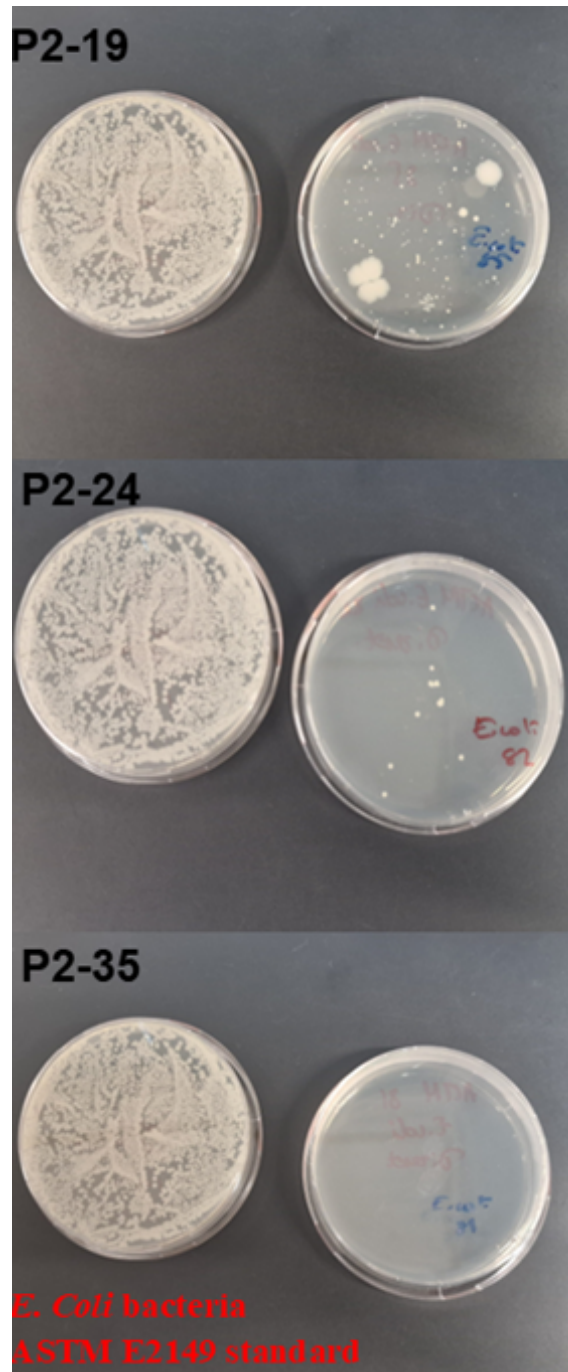


Figure 3.21 The right sample, coated with copolymer latexes, and the left control were assessed for their antibacterial efficacy of Gram negative bacteria by ASTM E2149 standard method

Tested coated materials exhibit antibacterial activity against both representative bacteria and meet the criteria, according to the ISO 22196 standard method. (Table 3.7, Table 3.8)

Sample	Microbial load (cfu/cm ²)	Reduction (%)	R
P1-19	< 10	> 99.9999	6.28
P1-24	< 10	> 99.9999	6.28
P1-35	< 10	> 99.9999	6.28
P2-19	1.16 × 10 ³	> 99.9930	4.22
P2-24	< 10	> 99.9999	6.28
P2-35	< 10	> 99.9999	6.28
Control (Untreated material)	2.98 × 10 ⁵ (0. hour)	1.92 × 10 ⁷ (24. hour)	—
Bacteria control	3.10 × 10 ⁵		

Table 3.7 Antibacterial test of copolymer latexes towards Gram-positive bacteria (*S. aureus* ATCC 65) by ISO 22196 standard method.

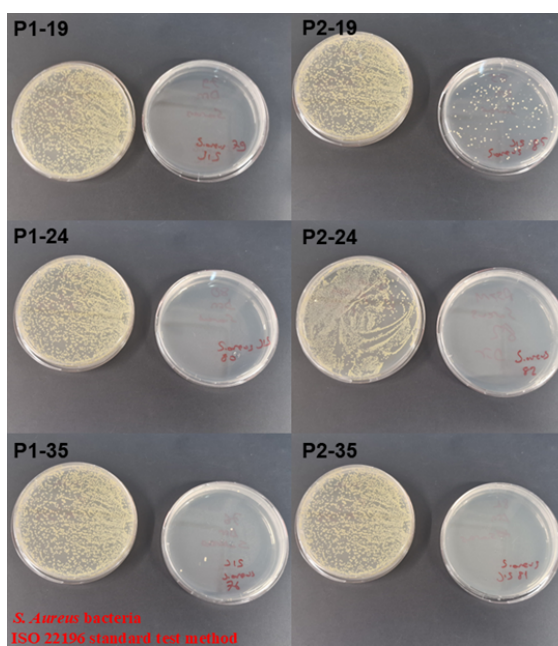


Figure 3.22 The right sample, coated with copolymer latexes, and the left control were assessed for their antibacterial efficacy of Gram positive bacteria by ISO 22196 standard method.

Sample	Microbial load (cfu/cm ²)	Reduction (%)	R
P1-19	< 10	> 99.9999	6.60
P1-24	< 10	> 99.9999	6.60
P1-35	< 10	> 99.9999	6.60
P2-19	2.90×10^3	> 99.9930	4.14
P2-24	< 10	> 99.9999	6.60
P2-35	< 10	> 99.9999	6.60
Control (Untreated material)	1.77×10^5 (0. hour)	4.00×10^7 (24. hour)	—
Bacteria control	3.10×10^5		

Table 3.8 Antibacterial test of copolymer latexes towards Gram-negative bacteria (*E. coli* ATCC 2592) by ISO 22196 standard method.

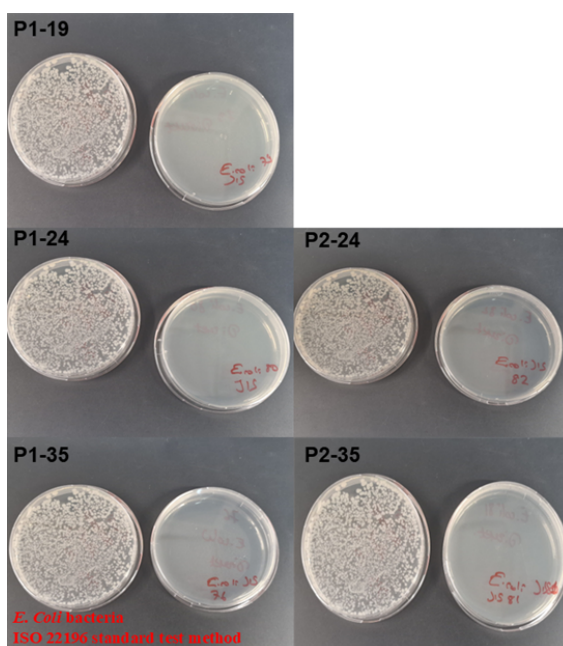


Figure 3.23 The right sample, coated with copolymer latexes, and the left control were assessed for their antibacterial efficacy of Gram-negative bacteria by ISO 22196 standard method.

3.10 Thermal Gravimetric Analysis

Thermal stability and weight loss of the emulsifiers and copolymer latex films were conducted by TGA analysis. Analysis was conducted between 25°C and 800°C with 10.0°C/min under nitrogen. Figures 3.24 and 3.25 indicate the time-dependent weight loss of non-ionic emulsifiers, cationic emulsifiers, and copolymer latex films.

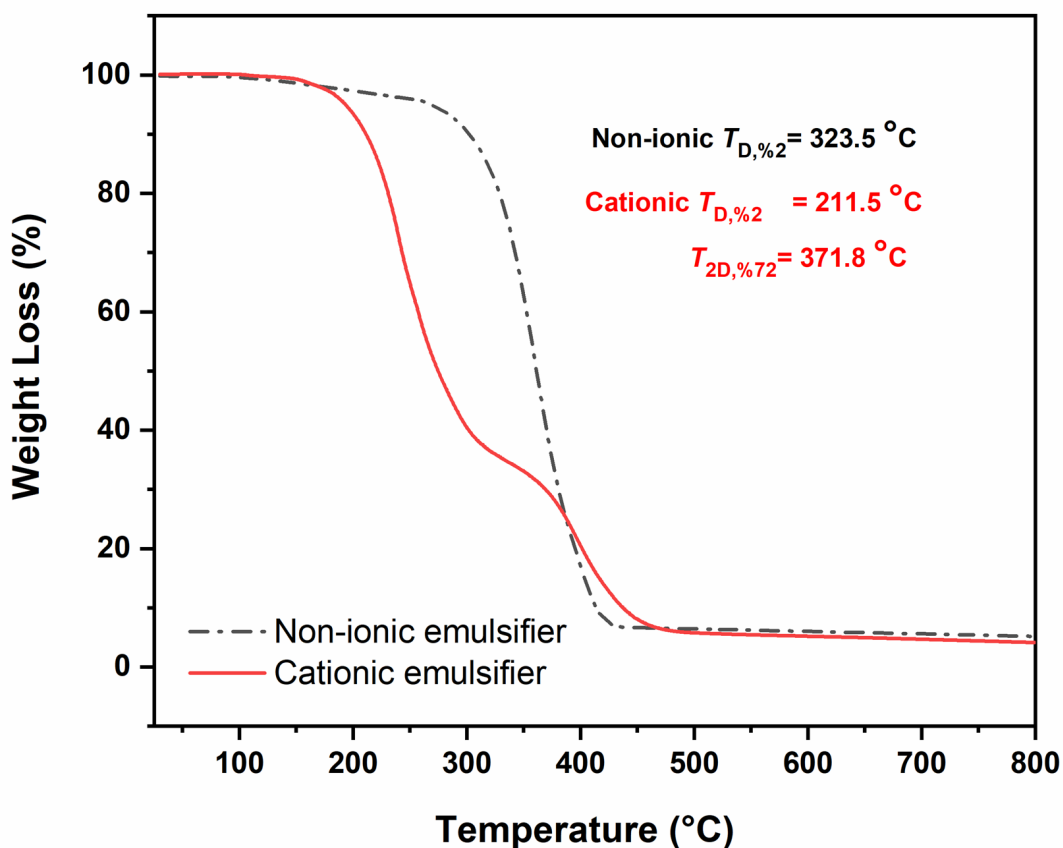


Figure 3.24 TGA analysis of a) non-ionic emulsifier and b) cationic emulsifier.

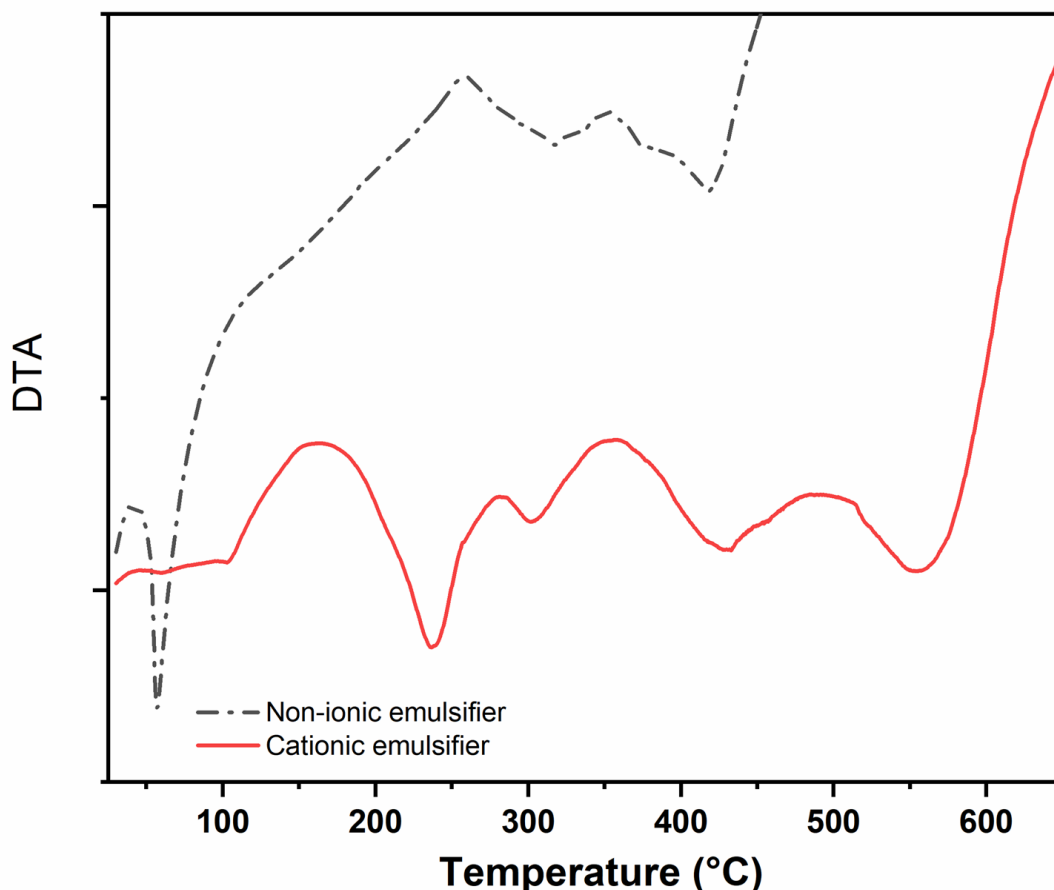


Figure 3.25 DTA analysis of a) non-ionic emulsifier and b) cationic emulsifier.

It can be seen in Fig. 3.24a that the 2% mass loss, which is below, 100°C can be ascribed as the removal of trapped solvents (toluene, ethyl acetate). Huang, Lu, Yeh, Lin & Tsai (2008) demonstrated that poly(maleic anhydride)-grafted polyethylene undergoes degradation in a single step 380 – 520°C (Ertuğral & Alkan (2020); KP, Thayyil, Binesh, Deshpande & Rajan (2018)). The small shoulder in the mass loss curve at 200°C and 300°C indicates the degradation of the maleic anhydride group (Ertuğral & Alkan (2020)). In a separate study, the thermogravimetric degradation of PEG 8000 showed a single-step degradation at 350 – 425°C (Sun et al. (2017)). Figure 3.24a shows no significant mass loss or degradation until about 320°C. The degradation 320 – 420°C corresponded to the degradation of the long PEG chain. Literature reports indicate that degradation of benzalkonium chloride occurs in a single step of weight loss, which begins at 180°C and is completed at 300°C (Huang & Nishinari (2001)). Similarly, polyvinylbenzylchloride decomposed in a single step of weight loss from 320 to 410°C (Meng & Hu (2008)). Figure 3.24b presents degradation of cationic emulsifier in two steps. The first weight loss occurs around 211°C, followed by a second decomposition step at approximately 371°C, which is exhibited

similarly with the thermal behavior in the literature.

As shown in figure 3.26, thermal degradation curves of copolymer latex films indicate a slower initial followed by a rapid degradation process, which follows a steps degradation mechanism, unlike the amount of the emulsifier type contained. The first weight losstage, between 198 – 250°C, indicates the decomposition of the cationic emulsifier. The second degradation stage 377 – 392°C was attributed to decomposition of styrene and non-ionic emulsifier.

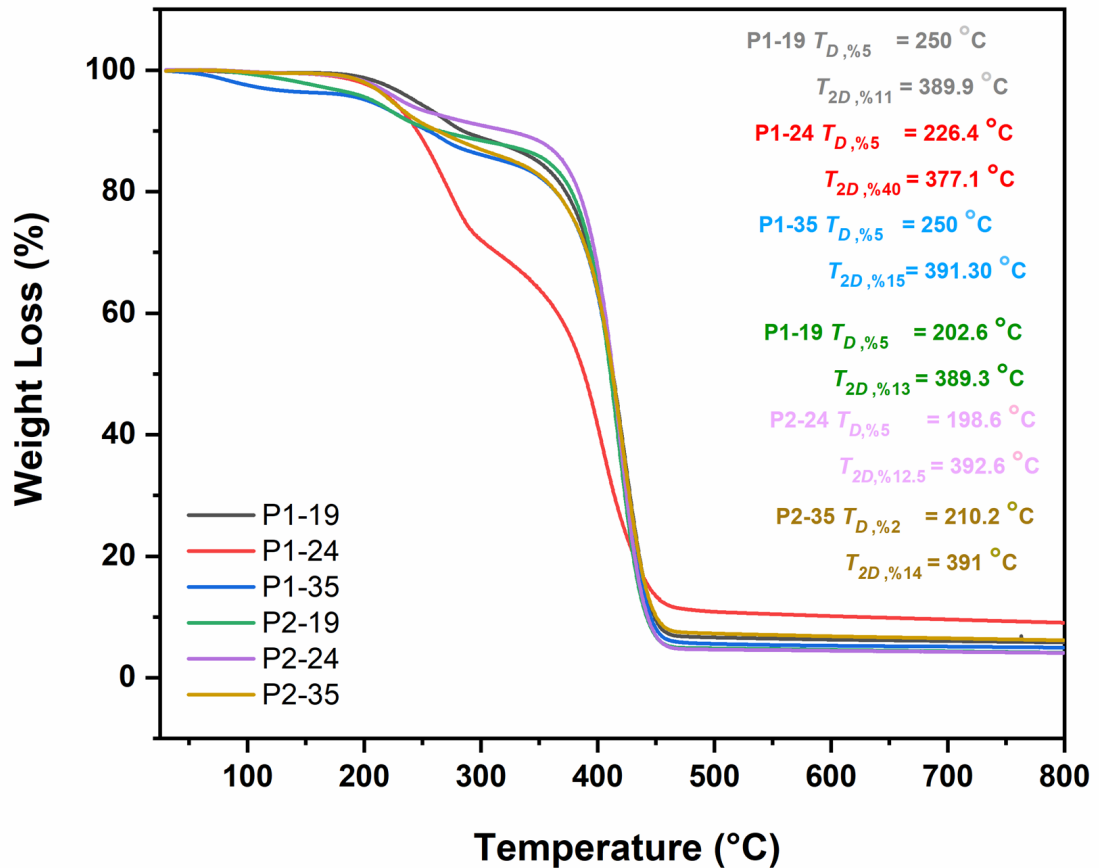


Figure 3.26 TGA analysis of copolymer latex films.

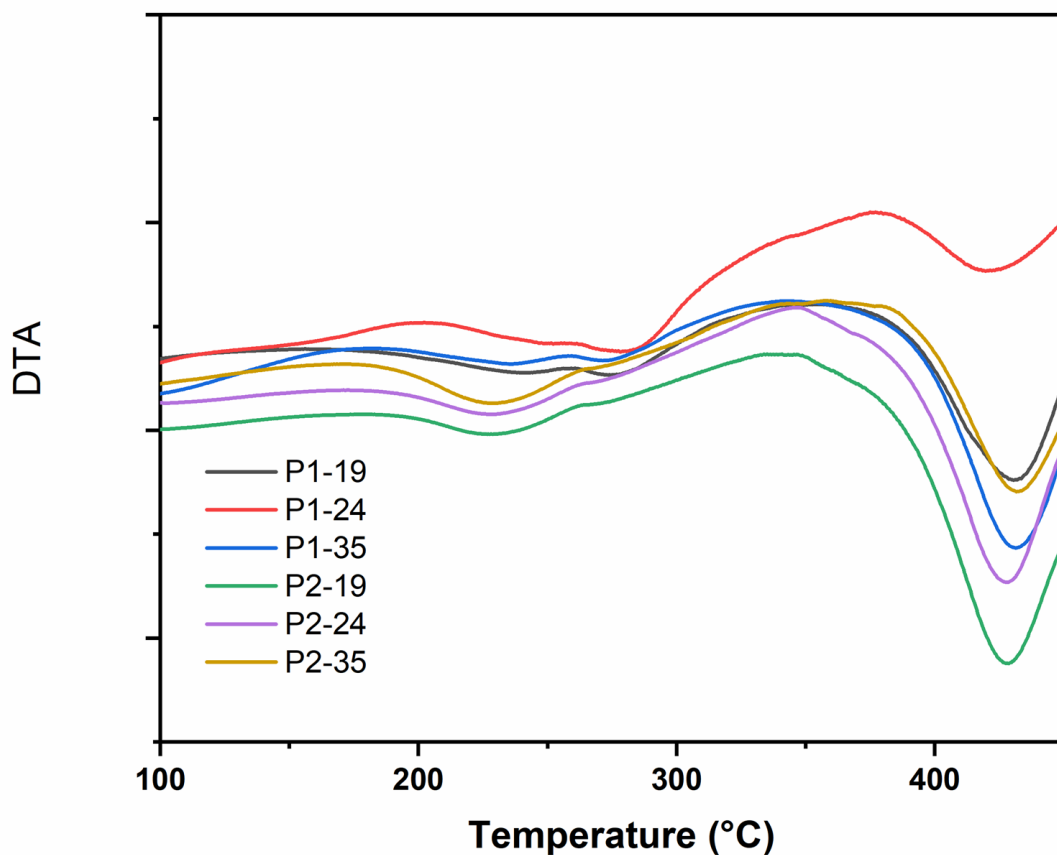


Figure 3.27 DTA analysis of copolymer latex films.

The weight loss of the samples is given in Table 3.9; It can be stated that P1-24 has better thermal stability compared to other films.

Samples	Overall weight loss (%)
P1-19	93.20
P1-24	90.04
P1-35	95.40
P2-19	95.60
P2-24	96.01
P2-35	91.02

Table 3.9 Weight loss of copolymer latex films in TGA.

The thermal properties of copolymer latex films were investigated in a range between -30 and 200°C in terms of glass transition temperature and melting points.

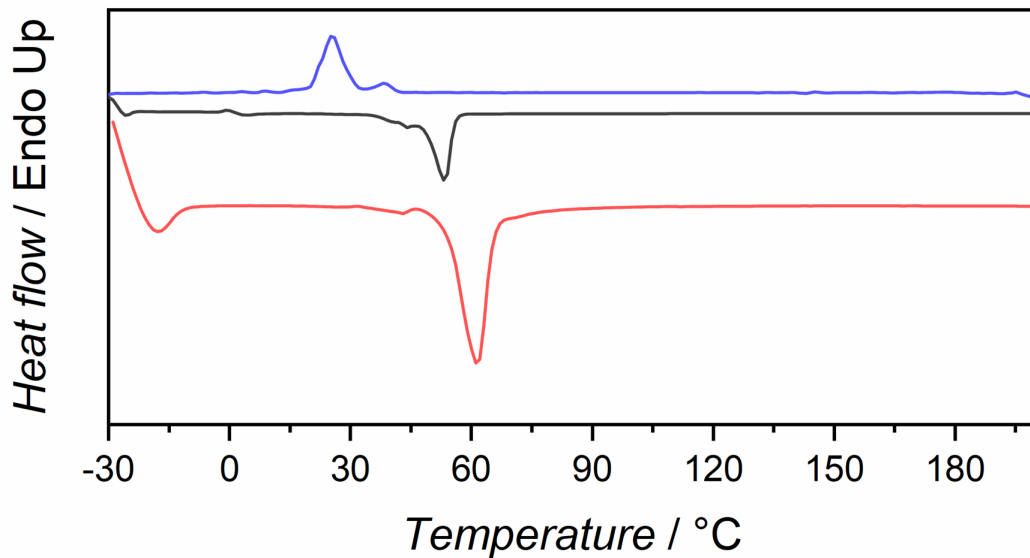


Figure 3.28 DSC curves of a) non-ionic emulsifier.

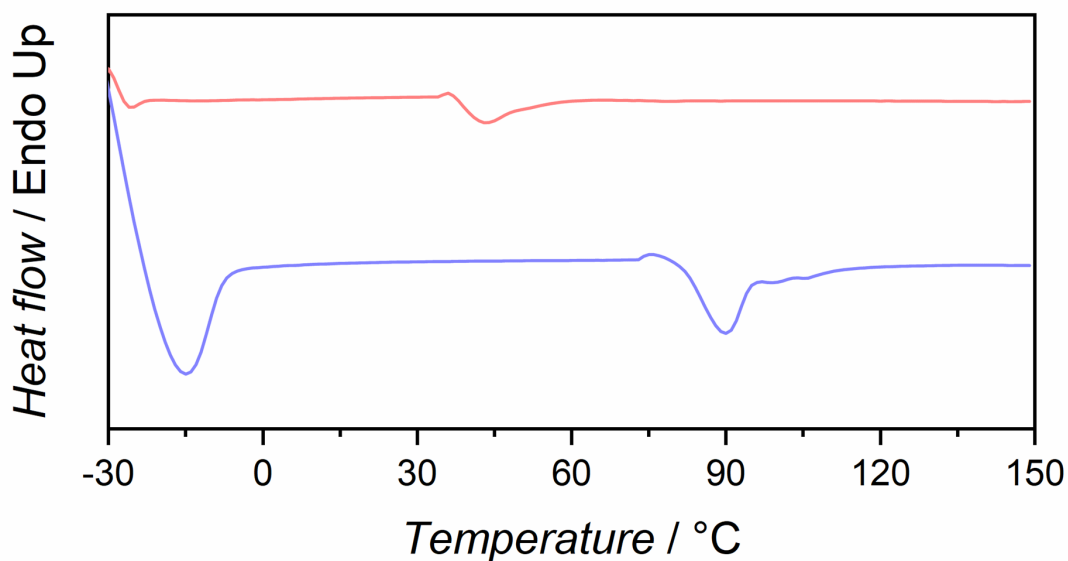


Figure 3.29 DSC curves of b) cationic emulsifier

Non-ionic emulsifier exhibits a sharp melting point at 53°C and shows a slight T_g at 0°C. It also displays two distinct crystallization points at 24°C and a smaller peak at 36°C, which corresponds to PEG 2500. The PEG unit of non-ionic emulsifier falls within a medium molecular weight between 1900 and 2100, consistent with literature values (KP et al. (2018)). For instance, maleic anhydride-modified PEG 6000 has exhibited a sharp melting point at 61°C and a crystallization temperature of 42°C (Wang & Wu (2017)). The cationic emulsifier exhibits a melting point at 44°C and T_g at -22°C, consistent with findings by KP et al. (2018), where benzalkonium

chloride exhibits a melting endotherm at 45°C and T_g at -43°C (Meng & Hu (2008)). As figured in 3.29, cationic emulsifiers show almost a sharp melting point at 46°C.

Figure 3.30 and 3.31 presents the DSC analysis of copolymer latex films with varying emulsifier contents (19-35% weight), revealing the glass transition and melting behavior of copolymer latex and emulsifier, respectively, between -30°C to 200°C. All samples show characteristic T_g peaks around -23°C and -14°C. During the second heating cycle, a sharp shoulder in the melting point is observed for P1-19, P2-19, P2-24, and P2-35, while sharp melting points are exhibited for P1-24 and P1-35. The melting peaks around 37°C and 47°C correspond to the cationic emulsifier, while 51°C those that 54°C are attributed to the non-ionic emulsifier. Although the efficiency of non-ionic emulsifiers in a polymer chain is higher, the melting point value of P1-24 exhibits between two separate melting . At the same time, P1-35 is closer to the non-ionic emulsifier, suggesting higher ionic emulsifier efficiency on points of emulsifiers. At the same time, P1-35 is closer to the non-ionic emulsifier, suggesting higher ionic emulsifier efficiency on the polymer chain. The DSC results for copolymer latex films show that the first heating scan differs from subsequent cycles, which can be attributed to the sample's different thermal history (Song, Lee, Woo, Sohn & Shin (2014)). As the PEG content increases, the T_m point value increases. Both non-ionic and cationic emulsifier contents significantly affect the T_m and T_g points, particularly shifting the T_g points of styrene (45°C) to the lower temperatures Wang & Wu (2017).

Another approach for Sun et al. (2017) This study demonstrates the substantial influence of emulsifier type and content on the thermal properties of latex films, with particular emphasis on how these components affect the glass transition and melting behavior. The shifts in T_g and T_m observed with varying emulsifier content are important for optimizing the thermal stability and processing conditions of the copolymer latex films.

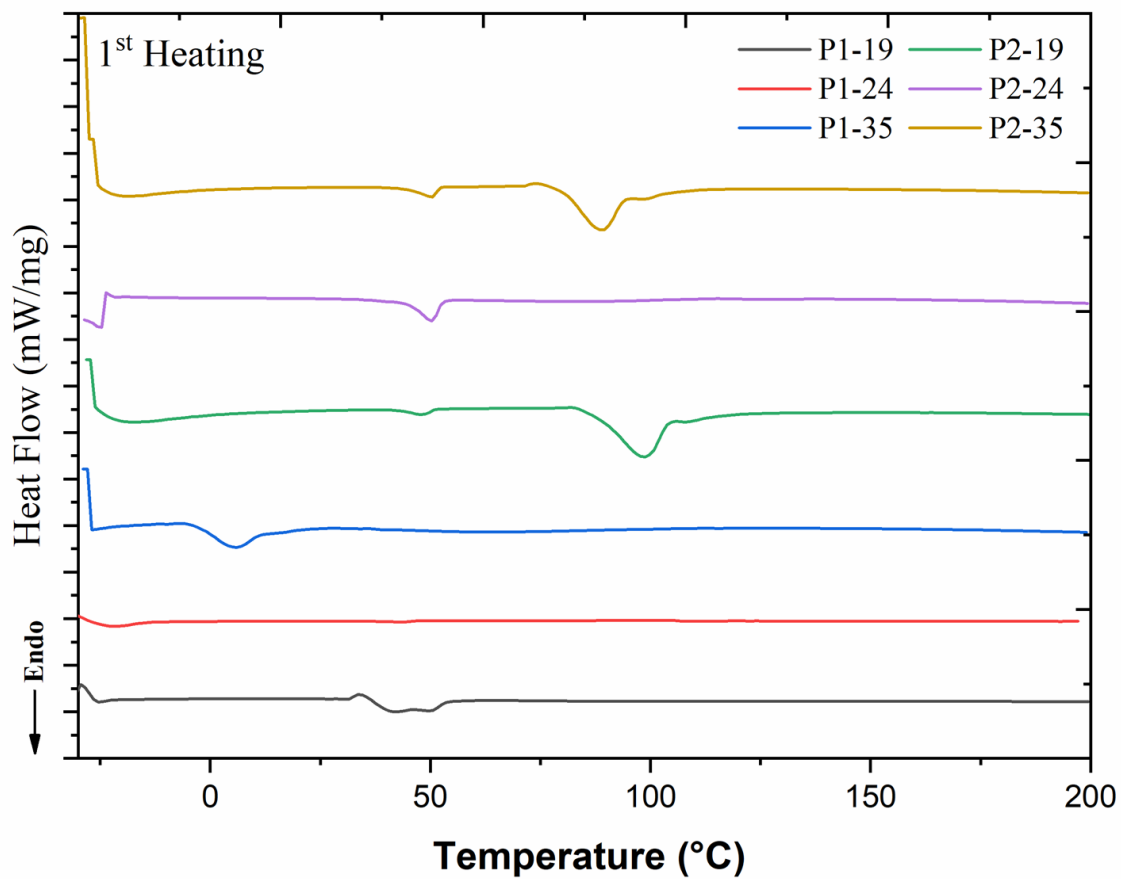


Figure 3.30 DSC curves of copolymer latex films a) 1st heating

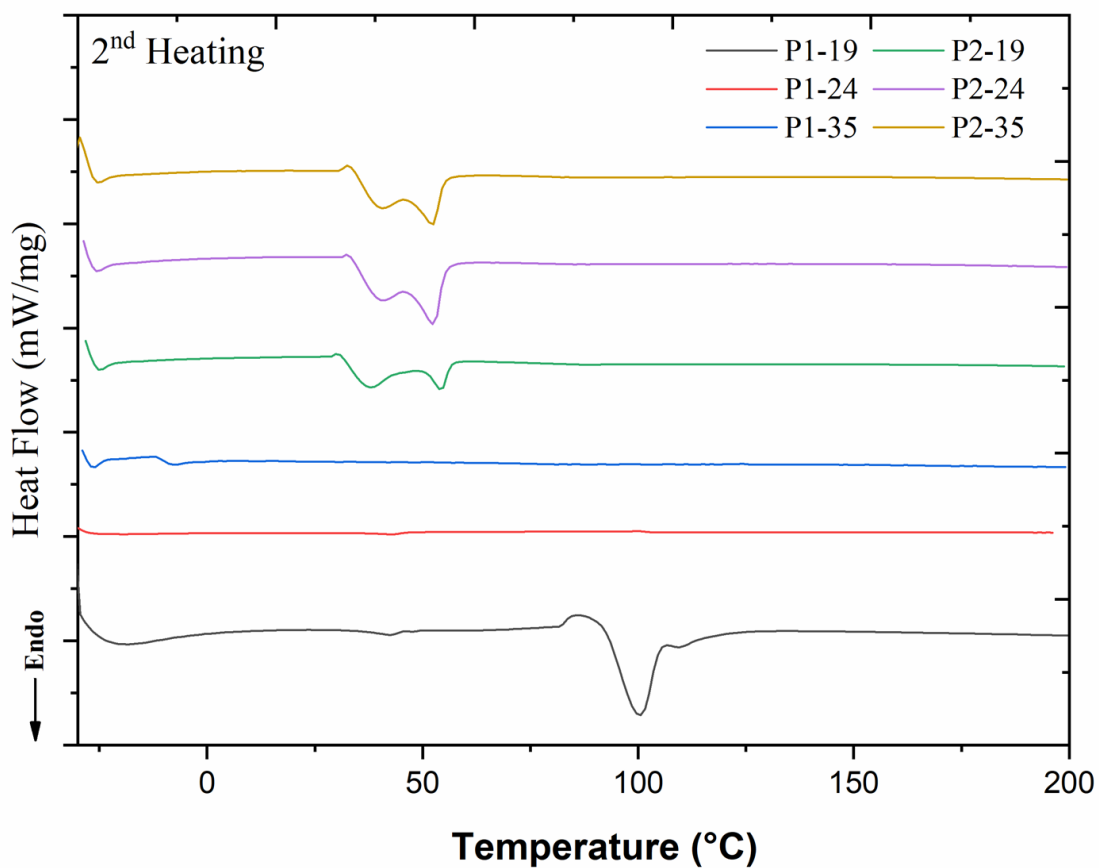


Figure 3.31 DSC curves of copolymer latex films b) 2nd heating

Samples	T _m (°C)	T _g (°C)
P1-19	42.2-51	-23
P1-24	43.9	-22
P1-35	50.8	-14
P2-19	37.7-54	-23
P2-24	41.3-52.6	-22
P2-35	41-52.2	-22

Table 3.10 Thermal properties of copolymer latex films.

4. CONCLUSION

This work reports the successful emulsion polymerization of styrene copolymer latexes exhibiting high molecular weight, good stability, and notable antibacterial properties. The results demonstrate that copolymer latexes synthesized using reactive non-ionic and cationic emulsifiers show enhanced antibacterial features, with the cationic emulsifiers playing a key role in this property. Among the formulations, P2-24 exhibited the highest monomer conversion, and a slightly elevated molecular weight compared to the other latexes. DLS analysis confirmed the durability of this formulation, with minimal changes in particle size distribution after 30 days of storage. SEM analysis revealed smooth and defect free surface morphology, and UV-Vis analysis further confirmed the exceptional optical transparency of the films.

The incorporation of the cationic emulsifier significantly enhanced the antibacterial properties against both Gram-positive and Gram-negative bacteria for latex films. This highlights the potential of these latexes for use in antimicrobial coating applications. Finally, P2-24 emerged as the most promising formulation due to its optimal balance of high conversion, stable molecular weight, excellent film formation, and superior antibacterial performance. This study demonstrates that reactive emulsifiers can produce stable, waterborne copolymer latexes suitable for clear coatings.

As an outlook, long-term studies investigating the non-migratory features of these latexes, through morphological analysis, could provide additional insights. This would expand the potential applications of these latexes across a broader range of industrial sectors.

BIBLIOGRAPHY

- Aramendia, E., Mallécol, J., Jeynes, C., Barandiaran, M. J., Keddie, J. L., & Asua, J. M. (2003). Distribution of surfactants near acrylic latex film surfaces: a comparison of conventional and reactive surfactants (surfmers). *Langmuir*, *19*(8), 3212–3221.
- Barboiu, V., Streba, E., Luca, C., Radu, I., & Grigoriu, G. E. (1998). Reactions on polymers with amine groups. v. addition of pyridine and imidazole groups with acetylenecarboxylic acids. *Journal of Polymer Science Part A: Polymer Chemistry*, *36*(10), 1615–1623.
- Chang, W., Liu, L., Zhang, J., Pan, Q., & Pei, M. (2009). Preparation and characterization of styrene/butyl acrylate emulsifier-free latex with 2-acrylamido-2-methyl propane sulfonic acid as a reactive emulsifier. *Journal of dispersion science and technology*, *30*(5), 639–642.
- Clogston, J. D. & Patri, A. K. (2011). Zeta potential measurement. *Characterization of nanoparticles intended for drug delivery*, 63–70.
- Ertuğral, T. G. & Alkan, C. (2020). Synthesis and characterization of maleic anhydride modified poly (ethylene glycol) as polymeric solid-solid phase change materials. *Sakarya University Journal of Science*, *24*(5), 1023–1028.
- Feng, J., Winnik, M. A., Shivers, R. R., & Clubb, B. (1995). Polymer blend latex films: morphology and transparency. *Macromolecules*, *28*(23), 7671–7682.
- Friberg, S. (1985). Polymeric stabilization of colloidal dispersions. *Journal of Dispersion Science and Technology*, *6*(4), 497–497.
- Goel, V., Beginn, U., Mourran, A., & Moller, M. (2008). ‘quat-primer’ polymers bearing cationic and reactive groups: Synthesis, characterization, and application. *Macromolecules*, *41*(21), 8187–8197.
- Hansen, F. & Ugelstad, J. (1978). Particle nucleation in emulsion polymerization. i. a theory for homogeneous nucleation. *Journal of Polymer Science: Polymer Chemistry Edition*, *16*(8), 1953–1979.
- Harkins, W. D. (1947). A general theory of the mechanism of emulsion polymerization1. *Journal of the American Chemical Society*, *69*(6), 1428–1444.
- Huang, J.-W., Lu, W.-C., Yeh, M.-Y., Lin, C.-H., & Tsai, I.-S. (2008). Unusual thermal degradation of maleic anhydride grafted polyethylene. *Polymer Engineering & Science*, *48*(8), 1550–1554.
- Huang, L. & Nishinari, K. (2001). Interaction between poly (ethylene glycol) and water as studied by differential scanning calorimetry. *Journal of Polymer Science Part B: Polymer Physics*, *39*(5), 496–506.
- KP, S. H., Thayyil, M. S., Binesh, M., Deshpande, S., & Rajan, V. K. (2018). Molecular dynamics in amorphous pharmaceutically important protic ionic liquid–benzalkonium chloride. *Journal of Molecular Liquids*, *251*, 487–491.
- Lovell, P. A. & Schork, F. J. (2020). Fundamentals of emulsion polymerization. *Biomacromolecules*, *21*(11), 4396–4441.
- Meng, Q. & Hu, J. (2008). A poly (ethylene glycol)-based smart phase change material. *Solar Energy Materials and Solar Cells*, *92*(10), 1260–1268.
- Mohapatra, S., Xian, J. L. L., Galvez-Rodriguez, A., Ekande, O. S., Drewes, J. E., & Gin, K. Y.-H. (2024). Photochemical fate of quaternary ammonium com-

- pounds (qacs) and degradation pathways predication through computational analysis. *Journal of Hazardous Materials*, 133483.
- Sardari, A. & Mannari, V. (2024). Emulsion polymerization process: effects of particle nucleation mechanism on properties of acrylic-styrene latex. *Journal of Coatings Technology and Research*, 1–14.
- Solyman, S. M., Elsharaky, E., & El-Tabey, A. E. (2018). Synthesize and characterization of new polymeric surfactants based on nonionic maleate surfmer by catalytic bulk copolymerization with methyl methacrylate. *Egyptian Journal of Petroleum*, 27(2), 257–264.
- Song, J.-M., Lee, S.-Y., Woo, H.-S., Sohn, J.-Y., & Shin, J. (2014). Thermal behavior of poly (vinylbenzyl chloride)-grafted poly (ethylene-co-tetrafluoroethylene) films. *Journal of Polymer Science Part B: Polymer Physics*, 52(7), 517–525.
- Steward, P., Hearn, J., & Wilkinson, M. (2000). An overview of polymer latex film formation and properties. *Advances in colloid and interface science*, 86(3), 195–267.
- Sun, Q., Yuan, Y., Zhang, H., Cao, X., & Sun, L. (2017). Thermal properties of polyethylene glycol/carbon microsphere composite as a novel phase change material. *Journal of Thermal Analysis and Calorimetry*, 130, 1741–1749.
- Szkurhan, A. R. & Georges, M. K. (2004). Stable free-radical emulsion polymerization. *Macromolecules*, 37(13), 4776–4782.
- Tsuji, S. & Kawaguchi, H. (2005). Self-assembly of poly (n-isopropylacrylamide)-carrying microspheres into two-dimensional colloidal arrays. *Langmuir*, 21(6), 2434–2437.
- Ugelstad, J. & Hansen, F. (1976). Kinetics and mechanism of emulsion polymerization. *Rubber chemistry and technology*, 49(3), 536–609.
- Wang, X. & Wu, P. (2017). Preparation of highly thermally conductive polymer composite at low filler content via a self-assembly process between polystyrene microspheres and boron nitride nanosheets. *ACS applied materials & interfaces*, 9(23), 19934–19944.
- Watrobska-Swietlikowska, D. (2020). Distribution of benzalkonium chloride into the aqueous phases of submicron dispersed systems: emulsions, aqueous lecithin dispersion and nanospheres. *Aaps Pharmscitech*, 21, 1–10.
- Yue, X., Zhang, R., Li, H., Su, M., Jin, X., & Qin, D. (2019). Loading and sustained release of benzyl ammonium chloride (bac) in nano-clays. *Materials*, 12(22), 3780.
- Zhang, Y., Wang, B., Dai, M., Pan, S., Zhang, F., & He, P. (2011). Studies on the preparation of stable and high solid content emulsifier-free poly (mma/ba/hea) latex with the addition of amps and characterization of the obtained copolymers. *Journal of Macromolecular Science, Part A*, 48(5), 409–415.